

# Consistent Quantization of Nearly Singular Superconducting Circuits

Martin Rymarz<sup>1,\*</sup> and David P. DiVincenzo<sup>1,2</sup>

<sup>1</sup>*JARA-Institute for Quantum Information, RWTH Aachen University, D-52056 Aachen, Germany*

<sup>2</sup>*Peter Grünberg Institute, Theoretical Nanoelectronics, Forschungszentrum Jülich, D-52425 Jülich, Germany*

 (Received 13 September 2022; revised 5 January 2023; accepted 17 March 2023; published 1 May 2023)

The theory of circuit quantum electrodynamics has successfully analyzed superconducting circuits on the basis of the classical Lagrangian, and the corresponding quantized Hamiltonian describing these circuits. In many simplified versions of these networks, the modeling involves a singular Lagrangian that employs Kirchhoff's laws to eliminate inherent constraints of the system. In this work, we demonstrate the failure of such singular theories for the quantization of realistic, nearly singular superconducting circuits. Instead, we rigorously prove the validity of a perturbative analysis within the Born-Oppenheimer approximation. In particular, we find that the limiting behavior of the low-energy dynamics obtained from the regularized approach exhibits a fixed-point structure flowing to one of a few universal fixed points as parasitic capacitance values go to zero. This singular limit of the regularized analysis is, in many cases, completely unlike the singular theory. Consequently, we conclude that classical network synthesis techniques which build on Kirchhoff's laws must be critically examined prior to applying circuit quantization.

DOI: [10.1103/PhysRevX.13.021017](https://doi.org/10.1103/PhysRevX.13.021017)

Subject Areas: Electronics, Quantum Physics,  
Quantum Information

## I. INTRODUCTION

Superconducting circuits facilitate a highly promising architecture for the realization of a universal quantum computer [1,2], whose potential to outperform a classical computer in special tasks [3–5] is the driving force of an entire area of research. However, although superconducting qubits have existed for more than two decades [6–8], state-of-the-art quantum technology is still too noisy to allow for accurate calculations of arbitrary length [9]. Many efforts are put into the improvement of currently existing superconducting qubits as well as into the invention and fabrication of entirely new designs. Purposeful design of new circuits has been successful; for instance, the  $0-\pi$  qubit [10–14] constitutes a prototypical example of an intrinsically noise-protected superconducting qubit that has recently been experimentally realized [15].

Theoretical work has been a successful contributor to this effort. Ideally, superconducting circuits are described by a lossless dynamics of a discrete set of degrees of freedom. These circuits are described classically on the

Hamiltonian level, where fluxes and charges are considered as pairs of conjugate variables. The quantization of these macroscopic Hamiltonians has been successful [16–19], with quantitatively accurate predictions of many observed phenomena.

It may be noted that more advanced superconducting qubit designs that strive for an inherent protection can be expected to have a large number of independent degrees of freedom [20]. In such systems, one often sees the emergence of a pronounced hierarchy of the involved energy (or time) scales. The consequences of such a hierarchy will be the subject of this paper.

The purposeful use of this hierarchy is one aspect of a set of four very simple design principles, which have enabled the large number of successful circuit designs that are in use today: (1) use only the standard lossless circuit elements, the capacitor and the inductor (obviously) avoiding resistors, (2) achieve long-distance coupling by transmission lines, but used in such a way that they again can be effectively represented by a small assembly of capacitors and inductors, (3) use metallization to, on purpose, make some node-to-node capacitances very large, while keeping many node-to-node capacitances at their small, parasitic values, resulting in a range of capacitance values of perhaps 7 orders of magnitude [21] (this is the hierarchy we study here), and (4) use linear as well as nonlinear inductors.

Of course, principle 4 is a centerpiece of qubit circuits, with the use of a particular nonlinearity, that given by the

\*martin.rymarz@rwth-aachen.de

*Published by the American Physical Society under the terms of the Creative Commons Attribution 4.0 International license. Further distribution of this work must maintain attribution to the author(s) and the published article's title, journal citation, and DOI.*

Josephson junction. In contrast to a linear inductance described by a linear current-versus-flux characteristic  $I = \phi/L$ , the Josephson nonlinear inductor has the two-terminal characteristic  $I = I_c \sin(2\pi\phi/\Phi_0)$  ( $\Phi_0 = h/2e$ ). The availability of this low-loss nonlinearity permits the quantum eigenspectrum of these circuits to be atomlike, in that it can make the  $|0\rangle - |1\rangle$  energy difference unique, making it possible to perform quantum-logic gates by resonant Rabi driving.

We show here that principles 3 and 4 interact in a novel and, potentially, dangerous way. A first, seemingly natural step in the analysis of circuits is, given the capacitance hierarchy of real structures, to declare a certain capacitance threshold  $C_{\text{th}}$ , and to set all capacitances below this value equal to zero. This considerably simplifies the analysis and leads to a straightforward way of conceptualizing very useful composite effective inductance structures, including the superinductor [11,22–26] and the superconducting nonlinear asymmetric inductive element (SNAIL) [27–29] to be discussed below.

This simplification often leads to an important consequence for the mechanics of the circuit. Adopting the common procedure of describing this mechanics using a Lagrangian  $\mathcal{L}$  with node fluxes  $\phi_i$  as dynamical variables [16–19], one finds that some dynamical variables can become constrained. A constrained variable is one whose conjugate variable  $\partial\mathcal{L}/\partial\dot{\phi}_i$  cannot be properly inverted to obtain  $\dot{\phi}_i$ , and whose classical dynamics is slaved to other independent variables, i.e.,  $\phi_1(t) = g(\phi_2(t), \phi_3(t), \dots)$ , at all times. Constrained (or “frozen”) variables are indeed considered a useful simplification in current treatments of superconducting circuits, singled out in currently available software [30].

Singular mechanics and its quantization have received considerable attention in modern physics. The first systematic treatments of singular Lagrangians and proposals for their quantization were proposed independently by Dirac and Bergmann in the early 1950s [31–36]. Since then, the proposed procedure of progressively identifying and classifying certain constraints of the system, known as the Dirac-Bergmann algorithm [37–39], has been frequently applied to various singular gauge theories. Often these theories are applied in cases where the singularity is viewed as fundamental, for example, when a particle is expected to have exactly zero mass. There also exist singular Lagrangians that approximate a limiting case of a nonsingular system, e.g., when a particle has very small but nonzero mass. We consider the circuit problem to be in the latter category: Capacitances play the role of masses, and, according to basic electrostatics, node-to-node capacitances are never exactly zero.

The Dirac-Bergmann algorithm can be worked out for general lossless electric networks. For the circuits considered in this work, the Dirac-Bergmann algorithm amounts to applying Kirchhoff’s current law, eliminating variables

by using basic series-combination rules. For example, the algorithm says that a series combination of inductances  $L_1$  and  $L_2$  can be replaced by a single inductance  $L_1 + L_2$  (thus neglecting any capacitance to the joining node). This indeed turns out to be correct from all points of view.

But, the Dirac-Bergmann algorithm makes predictions also for nonlinear circuits, i.e., involving Josephson elements. Do its predictions also agree with a “regularized” approach, in which one considers the limit as all small capacitances are taken to zero? The answer is, absolutely, no. A sign of trouble already appears when we consider a series combination of a linear inductance and a Josephson inductor. While the resulting effective inductor depends in detail on the parameters of the two elements, for certain parameters the effective inductive energy is predicted to be multivalued.

Suggestions exist in the literature for how such a multivaluedness should be interpreted; see the theory of “branched Hamiltonians” [40,41] (see also Appendix A). However, we find no existing approach that matches the result of regularizing the singularity by taking small capacitances  $C_s < C_{\text{th}}$  into account. Our result is in complete contrast to Dirac and Bergmann, where the effective Hamiltonian depends in detail on the parameters of the nonlinear element; in the regularized treatment, the result has the structure of a renormalization flow, in the sense that the limit  $C_s \rightarrow 0$  gives a universal result with only a few possible fixed points.

To understand this fixed-point structure more comprehensively, we find it valuable to adopt the point of view, perhaps due to Heaviside, stated routinely in many textbooks on electrical theory [42–44]: An inductor is a two-terminal element exhibiting an instantaneous relationship between current and flux  $I(t) = f(\phi(t))$ , with arbitrary function  $f(\cdot)$ ; see Fig. 1. While distinctions are made between bijective, current-controlled, and flux-controlled inductors (the Josephson characteristic is flux controlled), in all cases this generalized inductor is a proper energy storage device. Thus, such an element can be incorporated into a circuit Lagrangian for arbitrary  $f(\cdot)$  [45].

This generalization is highly valuable in that it reveals that there are generically three fixed points as  $C_s \rightarrow 0$ . They are exemplified by our simple series-combination scenario, in which a linear inductance  $L$  is in series with a nonlinear inductor with antisymmetric characteristic  $I \sim \text{sign}(\phi)|\phi|^\beta$ . The renormalization flow is determined by  $\beta$ . For all



FIG. 1. Lumped element symbol of a nonlinear inductor. In particular, a flux-controlled inductor relates the electric current  $I(t)$  flowing through it and the magnetic flux difference  $\phi(t) = \phi_2(t) - \phi_1(t)$  at its terminals [with  $\phi_i(t)$  being the time-integrated node voltages; cf. Eq. (3)] via  $I(t) = f(\phi(t))$ , with an arbitrary function  $f(\cdot)$ .

“sublinear” cases ( $0 < \beta < 1$ ), the flow erases the two elements from the circuit; i.e., they are replaced by an open circuit. For the “superlinear” cases ( $\beta > 1$ ), the flow results in the nonlinear element being replaced by a short circuit. The linear  $\beta = 1$  case is marginal, and it is the one case where the combination procedure given by Dirac and Bergmann is essentially correct.

The Josephson case is in the sublinear universality class and flows to the open-circuit fixed point. To show this, and to determine the universality class of a large set of  $f(\cdot)$ , we calculate as follows: (1) For sufficiently small  $C_s$ , the variable to be eliminated becomes “fast” and can be accurately dealt with using the Born-Oppenheimer approximation. (2) With suitable rescaling, the fast-variable Schrödinger equation is one in which one term can be treated perturbatively.

To prove that the flow goes to our fixed points, we must prove the convergence of the resulting perturbation problem. Particularly for the sublinear case, we successfully treat a large class of functions  $f(\cdot)$  dealing with the perturbation theory rigorously using primarily the Kato-Rellich theorem [47] as provided by Reed and Simon [48]. We cannot prove that all  $f(\cdot)$  flow to one of the fixed points; we find that the flow has additional complexities when nonsymmetric characteristics are studied. We also show an amusing example of a self-similar  $f(\cdot)$  for which the flow is successively attracted by two different fixed points as  $C_s \rightarrow 0$ , but never reaches either of them.

One can finally say that the physics of our results has to do with the diverging quantum fluctuations of the variables to be eliminated as  $C_s \rightarrow 0$ . This is the complete opposite of the Dirac-Bergmann treatment, in which these variables have no independent quantum fluctuations, being simply slaved to other variables in the circuit. But while these zero-point fluctuations diverge, the character of these divergences shows three different varieties, giving rise to the three fixed points that we identify.

The remainder of this paper is organized as follows. In Sec. II, we review both the concepts of singular Lagrangians and the application of the Dirac-Bergmann algorithm. Based on two concrete examples, we demonstrate that the results of the systematically applied Dirac-Bergmann algorithm have to be handled with care if the system is supposed to be quantized. In Sec. III, we analyze the series combination of a linear inductance and a generic nonlinear inductor, and we provide an expression for the effective replacement of this series combination. In particular, we compare the results obtained from the Dirac-Bergmann algorithm with the limiting case of the low-energy dynamics derived from the Born-Oppenheimer approximation after the inclusion of small parasitic capacitances that lift the singularity of the system. In Sec. IV, we revise the frequently used single-phase approximation for the simplified analysis of arrays of Josephson junctions. We show that such a single-phase approximation is akin to the

application of the Dirac-Bergmann algorithm although an opposite limit of capacitances is considered. In particular, we provide a leading-order correction term to the single-phase approximation due to the finite intrinsic capacitances of the Josephson junctions. Finally, we summarize our results and provide a perspective for possible future work in Sec. V.

## II. SINGULAR SUPERCONDUCTING CIRCUITS AND THE DIRAC-BERGMANN ALGORITHM

The theory of circuit quantum electrodynamics [16–19] provides a very powerful tool for the description of superconducting circuits. Generally, it starts with a circuit modeling the electrical network under consideration. With a particular choice of variables, each circuit element usually can be associated with a contribution to the total Lagrangian describing the system [49]. After the assembly of the total Lagrangian, a Legendre transformation converts the Lagrangian formalism to the Hamiltonian formalism, which, in turn, is the starting point for a quantized theory. However, depending on both the physical precision and the details of the model that describes the system, the Legendre transformation is not always applicable, viz., invertible. Given a Lagrangian  $\mathcal{L}(\{x_i\}, \{\dot{x}_i\}, t)$ , which depends on generalized positions  $x_i$ , generalized velocities  $\dot{x}_i = dx_i/dt$ , and time  $t$ , the canonical momenta are defined as  $p_i = \partial\mathcal{L}/\partial\dot{x}_i$  and the corresponding Hamiltonian

$$H(\{x_i\}, \{p_i\}, t) = \sum_i p_i \dot{x}_i - \mathcal{L}(\{x_i\}, \{\dot{x}_i\}, t) \quad (1)$$

must be expressed as a function of  $x_i$ ,  $p_i$ , and  $t$ . In this process, the correct application of the Legendre transformation requires that every generalized velocity can be expressed as function of the generalized positions, the conjugate momenta, and the time, i.e.,

$$\dot{x}_i \equiv \dot{x}_i(\{x_j\}, \{p_j\}, t). \quad (2)$$

If it is not possible to obtain such a functional dependence for each generalized velocity, the Lagrangian is said to be singular, and a Legendre transformation is not well defined and thus not applicable. The terminology arises from the observation that for many physical systems, the Lagrangian contains a kinetic part that is quadratic in the generalized velocities, and solving for the velocities as in Eq. (2) corresponds to the inversion of a quadratic coupling matrix, which is not possible if this matrix is singular [50].

Accordingly, we refer to a superconducting circuit as singular if it is described by a singular Lagrangian. A singular Lagrangian implies that the physical system that is described has some underlying constraints [31–39] and that the canonical variables  $x_i$  and  $p_j$  within the Hamiltonian

description are not independent as assumed for the application of the variational principle. In particular, the classical phase-space variables are no longer necessarily canonical as the constraints restrict the dynamics to a subspace of the entire phase space. We stress that it might depend on the level of details of the system's description and on the choice of variables whether the corresponding Lagrangian is singular or not, as will be seen in examples below.

As elaborated in Refs. [31–39], a possible strategy to derive a quantized theory on a Hamiltonian level, starting from a singular Lagrangian, is accomplished by determining and classifying the system's underlying constraints and involves a subsequent reduction of the number of variables, remaining with independent variables only. This, however, is accompanied by a redefinition of the conventional Poisson brackets—defining the Dirac brackets—and hence, of the commutator in quantum mechanics as well. In general, this approach, which is known as the Dirac-Bergmann algorithm, can be rather involved, even for seemingly simple systems [51]. However, as pointed out by Dirac [36], the arguably simplest class of singular Lagrangians is the one in which one generalized momentum vanishes, say,  $p_1 = 0$ , while the corresponding generalized position can be expressed as a function of all the other canonical variables, i.e.,  $x_1 \equiv x_1(\{x_i\}_{i \neq 1}, \{q_i\}_{i \neq 1}, t)$ . In this case,  $x_1$  can be substituted in the Hamiltonian such that this degree of freedom can be discarded.

In the remainder of the paper, we focus on this simple class of singular Lagrangians in the setting of circuit quantization. In this context, the generalized positions are usually taken to be the magnetic fluxes associated with the nodes of the circuit,

$$\phi_i = \int_{t_0}^t dt' V_i(t'), \quad (3)$$

where  $V_i(t')$  is the voltage of the  $i$ th node with respect to ground [55]. For singular superconducting circuits, which are described by a Lagrangian that gives rise to vanishing generalized momenta, a full algebraic application of the Dirac-Bergmann algorithm can be worked out (including the systematic description of nonreciprocal superconducting circuits) [57,58], leading to a circuit Hamiltonian. But note that, as detailed later in this paper, we find this Dirac-Bergmann Hamiltonian to be an incorrect description of the circuit dynamics in many cases.

In order to get familiar with the Dirac-Bergmann algorithm in its arguably simplest form, and to indicate its limitations when applied to describe realistic superconducting circuits, we analyze two exemplary electrical networks that give rise to singular Lagrangians.

### A. Addition of linear inductances in series

First, we consider an apparently “trivial” example, a series combination of two linear inductances  $L_1$  and  $L_2$  that

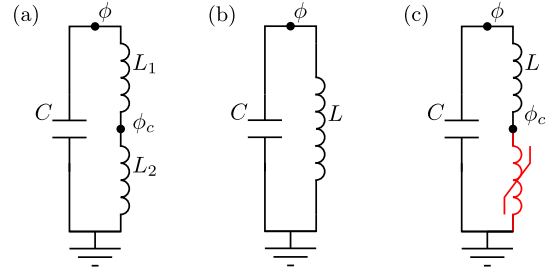


FIG. 2. (a) Series combination of two linear inductances  $L_1$  and  $L_2$  with a shunting capacitance  $C$ , and (b) the effective equivalent  $LC$  circuit obtained by eliminating the constrained variable and adding the inductances  $L = L_1 + L_2$ . (c) Series combination of a linear inductance  $L$  and a nonlinear inductor (red) with a shunting capacitance  $C$ .

is shunted by a capacitance  $C$ ; see Fig. 2(a). The two-dimensional Lagrangian of this electrical network

$$\mathcal{L} = \frac{C\dot{\phi}^2}{2} - \frac{(\phi - \phi_c)^2}{2L_1} - \frac{\phi_c^2}{2L_2} \quad (4)$$

is singular because one cannot solve for the generalized velocity  $\dot{\phi}_c$  as a function of the generalized positions and momenta. However, since  $\dot{\phi}_c$  does not appear in the Lagrangian, we find that the corresponding generalized conjugate momentum vanishes, i.e.,  $Q_c = \partial\mathcal{L}/\partial\dot{\phi}_c = 0$ . Exploiting the classical Euler-Lagrange equation of motion for the  $\phi_c$  degree of freedom,

$$0 = \frac{d}{dt} \left( \frac{\partial\mathcal{L}}{\partial\dot{\phi}_c} \right) - \frac{\partial\mathcal{L}}{\partial\phi_c}, \quad (5)$$

we find the holonomic constraint

$$\phi_c = \frac{L_2}{L_1 + L_2} \phi, \quad (6)$$

which essentially is Kirchhoff's current conservation law at the node  $\phi_c$ . Inserting this expression in the Lagrangian in Eq. (4) renders it one dimensional and regular,

$$\mathcal{L} = \frac{C\dot{\phi}^2}{2} - \frac{\phi^2}{2L}, \quad (7)$$

with the total inductance  $L = L_1 + L_2$ . Thus, the elimination of the constrained variable  $\phi_c$  reproduces what one would expect, the addition of two inductances in a series connection. This shows that the circuit in Fig. 2(a) is effectively equivalent to an ordinary  $LC$  resonator; see Fig. 2(b). Finally, defining the conjugate charge  $Q = \partial\mathcal{L}/\partial\dot{\phi} = C\dot{\phi}$ , the Legendre transformation is applicable and results in the harmonic-oscillator Hamiltonian,

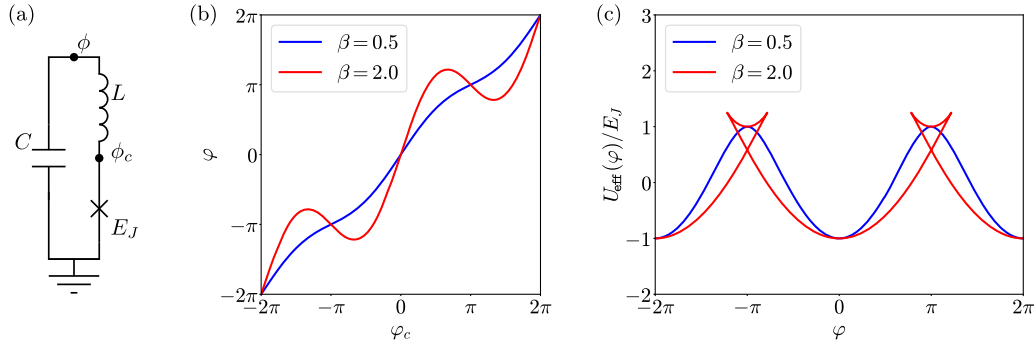


FIG. 3. Series combination of a linear inductance  $L$  and a Josephson junction  $E_J$  with a shunting capacitance  $C$ . (a) Circuit model. (b) Constraint relating the rescaled flux variables  $\varphi$  and  $\varphi_c$  [see Eq. (13)] for the different cases  $\beta \leq 1$  (blue) and  $\beta > 1$  (red), in which the constrained variable  $\varphi_c(\varphi)$  is either a well-defined function of  $\varphi$  or multivalued, respectively. (c) Effective one-dimensional potential [cf. Eq. (11)] obtained by substituting the constrained variable for the different cases  $\beta \leq 1$  (blue) and  $\beta > 1$  (red), in which  $U_{\text{eff}}(\varphi)$  is either a well-defined function of  $\varphi$  or multivalued, respectively.

$$H = \frac{Q^2}{2C} + \frac{\phi^2}{2L}, \quad (8)$$

which is quantized by imposing the canonical commutation relation  $[\phi, Q] = i\hbar$ .

This analysis demonstrates the application of the Dirac-Bergmann algorithm for a simple linear system, and the resulting total inductance  $L$  agrees with the well-known series-combination formula. If, however, the system is not linear, the Dirac-Bergmann algorithm will possibly result in a bizarre description of the dynamics. In the following, we highlight emerging inconsistencies in the Dirac-Bergmann algorithm by replacing one of the linear inductances with a nonlinear inductor—specifically, a Josephson junction.

### B. Addition of a linear and a nonlinear inductor in series

In the previous subsection, we consider a system with a constraint in the form of a one-to-one functional dependence between variables; see Eq. (6). However, the effective description of singular electrical networks might involve constraints of a different type as well. In this subsection, we demonstrate the possible emergence of multivalued constraints. In particular, we consider a series combination of a linear inductance  $L$  and a generic nonlinear inductor that is shunted by a capacitance  $C$ ; see Fig. 2(c).

The Lagrangian of the electrical network,

$$\mathcal{L} = \frac{C\dot{\phi}^2}{2} - \frac{(\phi - \phi_c)^2}{2L} - U_{\text{NL}}(\phi_c), \quad (9)$$

in which  $U_{\text{NL}}(\phi_c)$  describes the nonlinear inductor, is singular because it does not contain the generalized velocity  $\dot{\phi}_c$ , and, as a consequence, the associated generalized momentum vanishes. For the Lagrangian in Eq. (9), the Dirac-Bergmann algorithm effectively reduces to an evaluation of the classical Euler-Lagrange equation of

motion, i.e., Kirchoff's law of current conservation, for the  $\phi_c$  degree of freedom in order to eliminate it. Thus, setting the current through the linear inductor equal to that through the nonlinear one, we find the constraint

$$\phi = \phi_c + LU'_{\text{NL}}(\phi_c), \quad (10)$$

which must be inverted in order to obtain the functional dependence  $\phi_c(\phi)$ . Then, after eliminating the constrained variable  $\phi_c$  in the Lagrangian, the series combination of both the inductors can be replaced by an effective inductor that is described by the effective potential

$$U_{\text{eff}}(\phi) = \frac{[\phi - \phi_c(\phi)]^2}{2L} + U_{\text{NL}}[\phi_c(\phi)]. \quad (11)$$

By construction, the resulting Hamiltonian of the initially singular system

$$H_s = \frac{Q^2}{2C} + U_{\text{eff}}(\phi) \quad (12)$$

depends on one pair of conjugate variables only. However, as we show in the following, both the classical Hamiltonian description of the system as well as its quantization is not always straightforward.

To this end, we specify the nonlinear inductor as a Josephson junction with Josephson energy  $E_J$ ; i.e., we set  $U_{\text{NL}}(\phi_c) = -E_J \cos(2\pi\phi_c/\Phi_0)$ . The corresponding total circuit is shown in Fig. 3(a). After introducing the rescaled phase variables  $\varphi = 2\pi\phi/\Phi_0$ ,  $\varphi_c = 2\pi\phi_c/\Phi_0$ , and the screening parameter  $\beta = LE_J(2\pi/\Phi_0)^2$  [59], Eq. (10) reduces to Kepler's transcendental equation [60]

$$\varphi = \varphi_c + \beta \sin(\varphi_c), \quad (13)$$

which can be inverted numerically in order to solve for the constrained variable  $\varphi_c \equiv \varphi_c(\varphi)$ . Note that for  $\beta \leq 1$ , the

right-hand side of Eq. (13) is strictly monotonically increasing as  $\varphi_c$  increases. However, for  $\beta > 1$ , it can be separated into infinitely many regimes in which it is either monotonically increasing or decreasing, respectively; see Fig. 3(b).

As a result, for  $\beta \leq 1$ , the constrained variable  $\varphi_c$  is a well-defined single-valued function of  $\varphi$ , whereas it is multivalued for  $\beta > 1$ . In the latter case, for a given value of  $\varphi$ , there might exist several values of  $\varphi_c$  satisfying the constraint in Eq. (13). Consequently, while the effective potential  $U_{\text{eff}}(\varphi)$  [cf. Eq. (11)] can be single valued, it can also be multivalued, depending on the value of  $\beta$  [57,61]; see Fig. 3(c).

In the single-valued case ( $\beta \leq 1$ ), the Hamiltonian  $H_s$  in Eq. (12) is a mathematically well-defined function of a pair of two conjugate variables, and it can be used in the usual way to describe the dynamics of the system [57,61]. In particular, a quantized description is obtained by promoting the canonical variables to operators and imposing the canonical commutation relation  $[\phi, Q] = i\hbar$ .

In contrast, in the multivalued case ( $\beta > 1$ ), the alternative might be to describe the system by a so-called branched Hamiltonian [40,41], but both the classical as well as the quantum description become subtle. Branched Hamiltonians emerge in various other contexts outside of electrical network theory, e.g., in extensions of Einstein's theory of gravitation [62] or in effective models of systems with finite response times [63]. All branched Hamiltonians have in common that the system is not uniquely described by its phase-space coordinates; one requires further information to determine the state of the system. As a consequence, the classical motion of the system might not be predictable for a given set of initial variables [40].

As we show in Appendix A, for the electric network in Fig. 3(a), the multivaluedness of the Hamiltonian can be avoided at the expense of working with nonsymplectic coordinates.

The aim of the present work, however, is not to provide the general description of systems that potentially involve branched Hamiltonians. Instead, focusing on the quantized description of electrical networks, we note that from the point of view of electrostatics, nonzero (“parasitic”) capacitances occur between every node of a physical network [64], e.g., those of Josephson junctions, which, in practical realizations, always exist [65]. Thus, a more physical description of the system renders the Lagrangian regular, and, within this approach, the physical origin and interpretation of the multivaluedness becomes clear as the individual branches of the Hamiltonian correspond to classical (meta)stable points. But the limit of small but finite capacitances throughout the network reveals a qualitative mismatch between the effective dynamics of the system and that obtained from the Dirac-Bergmann algorithm applied to the singular counterpart [57].

### III. FAILURE OF THE DIRAC-BERGMANN ALGORITHM

In the previous section, we apply the Dirac-Bergmann algorithm, which reduces to an evaluation of Kirchhoff's current conservation law, to derive the Hamiltonian description of two simple superconducting circuits. For singular circuits with nonlinearities, however, the system's quantum dynamics resulting from this approach differs from a more appropriate treatment in which the singularities are lifted. In electrical networks, the singularity of the capacitance matrix is lifted by taking into account the small but finite intrinsic (or parasitic) capacitance of one or several network elements in the corresponding branch of the circuit. In this section, we determine in detail the discrepancy mentioned above between the singular and the regular approach, and we classify different types of nonlinearities. Our results justify the conclusion that one should not use Kirchhoff's current law to eliminate variables in the Lagrangian.

To provide a simple example that demonstrates the failure of the Dirac-Bergmann algorithm when applied to electrical networks, we consider the series combination of a linear inductance  $L$  and a generic nonlinear inductor with intrinsic capacitance  $C'$ , all in parallel with a total shunting capacitance  $C$ ; see Fig. 4.

In the following, we analyze and compare the two cases: (1) absent intrinsic capacitance  $C' = 0$  indicating the application of the Dirac-Bergmann algorithm and (2) extremely small but nonzero intrinsic capacitance  $C' > 0$ . In the first case, the Lagrangian of the circuit

$$\mathcal{L} = \frac{C\dot{\phi}^2}{2} + \frac{C'\dot{\phi}_c^2}{2} - \frac{(\phi - \phi_c)^2}{2L} - U_{\text{NL}}(\phi_c) \quad (14)$$

is singular, while in the second case it is regular. In particular, we allow the nonlinear inductor to be a generic flux-controlled inductor [42–44] that can be modeled via the potential  $U_{\text{NL}}(\phi_c)$ , which we do not further specify at this point.

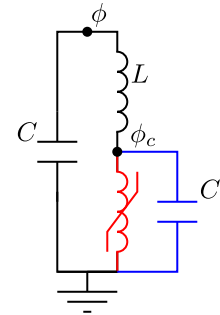


FIG. 4. Series combination of a linear inductance  $L$  and a nonlinear inductor (red) in parallel to a shunting capacitance  $C$ . The blue branch highlights the intrinsic capacitance  $C'$  of the nonlinear inductor, which we consider to be either vanishingly small (regular case) or absent (singular case).

The treatment of the singular case is already presented in Sec. II B. There, we also discuss the potential ambiguities in the construction of the effective potential  $U_{\text{eff}}(\phi)$  in Eq. (11). In the remainder of this work, the effective potential of the singular system will serve for a comparison with the limiting behavior of the regular case, which we analyze next.

### A. Approaching the singular limit: Born-Oppenheimer analysis

The consideration of nonzero but finite values of  $C'$  (see Fig. 4) is motivated by the observation that any physical realization of a network element contains some residual intrinsic or stray capacitance. For  $C' > 0$ , the Lagrangian in Eq. (14) describing the circuit shown in Fig. 4 is regular, and the Hamiltonian is straightforwardly obtained via an ordinary Legendre transformation resulting in

$$H_r = \frac{Q^2}{2C} + \frac{Q_c^2}{2C'} + \frac{(\phi - \phi_c)^2}{2L} + U_{\text{NL}}(\phi_c). \quad (15)$$

Here,  $\phi, Q$  and  $\phi_c, Q_c$  denote two independent pairs of conjugate variables, and  $H_r$  is quantized by imposing the canonical commutation relations  $[\phi_{(c)}, Q_{(c)}] = i\hbar$ .

In what follows, we compare the Hamiltonian of the regular circuit ( $H_r$  for  $C' > 0$ ) with that of the singular one ( $H_s$  for  $C' = 0$ ), and thus, we consider the limit of vanishingly small but finite  $C'$  in the regular system. We immediately note that  $H_r$  is two dimensional, whereas  $H_s$  describes the dynamics of 1 effective degree of freedom only. The fact that models with different numbers of dynamical variables could describe the same system can be understood by the observation that for  $C'/C \ll 1$  the timescales on which the dynamics of  $\phi$  and  $\phi_c$  change, as mediated by  $H_r$ , are vastly different.

In light of this, the Born-Oppenheimer approximation [66,67] will allow us to derive an effective low-energy Hamiltonian as a function of  $\phi$  and  $Q$  only. To this end, we first solve the stationary Schrödinger equation associated with the fast degree of freedom  $\phi_c$  for fixed values of  $\phi$  and  $Q$ . Thus, we identify the fast part [68] of  $H_r$  as

$$H_{\text{fast}} = \frac{Q_c^2}{2C'} + \frac{(\phi - \phi_c)^2}{2L} + U_{\text{NL}}(\phi_c), \quad (16)$$

and we solve

$$H_{\text{fast}}\psi_{\phi,n}(\phi_c) = E_{\phi,n}\psi_{\phi,n}(\phi_c) \quad (17)$$

for the eigenstates  $\psi_{\phi,n}(\phi_c)$  and the associated eigenenergies  $E_{\phi,n}$ , which both are labeled by  $n \in \mathbb{N}_0$  and parametrized by  $\phi$ . The ground-state energy ( $n = 0$ ) is then considered as an effective low-energy potential for the slow

variable  $\phi$ , whose dynamics is captured by the effective Hamiltonian

$$H_{r,\text{eff}} = \frac{Q^2}{2C} + U_{\text{BO}}(\phi), \quad (18)$$

with the Born-Oppenheimer potential that we define as

$$U_{\text{BO}}(\phi) = E_{\phi,0} - E_{0,0}. \quad (19)$$

Here, we choose the energy offset of  $U_{\text{BO}}(\phi)$  such that  $U_{\text{BO}}(0) = 0$  in order to avoid divergent additive constants.

In summary, the Born-Oppenheimer approximation provides an effective Hamiltonian  $H_{r,\text{eff}}$  for the regular case ( $C' > 0$ ), which is suitable for a comparison with  $H_s$  that is obtained in the singular case ( $C' = 0$ ). Note that the Born-Oppenheimer approximation becomes more accurate the smaller the ratio  $C'/C$ , which is exactly the regime of interest for the aforementioned comparison.

### B. Types of network branches leading to the failure of the Dirac-Bergmann algorithm

In the following, we evaluate the Born-Oppenheimer potential for a generic nonlinear inductor. Unless stated otherwise, we generally restrict our considerations to potentials  $U_{\text{NL}}(\phi_c)$  that are Riemann integrable on any finite domain, and that are symmetric in  $\phi_c$ , i.e.,  $U_{\text{NL}}(\phi_c) = U_{\text{NL}}(-\phi_c)$ , and that do not diverge for  $|\phi_c| < \infty$ . Furthermore, we assume that the nonlinear inductor can be categorized into one of the following three types, depending on the behavior of its potential for large values of  $\phi_c$  [69]:

- (1) Type 1 (sublinear [70]):
  - (a)  $U_{\text{NL}}(\phi_c) = U_{\text{NL}}(-\phi_c)$ ,  
 $\exists \gamma \in (0, 2) : \lim_{\phi_c \rightarrow \pm\infty} U_{\text{NL}}(\phi_c)/|\phi_c|^\gamma = 0$
  - (b)  $U_{\text{NL}}(\phi_c) \neq U_{\text{NL}}(-\phi_c)$ ,  
 $\exists \gamma \in (0, 1) : \lim_{\phi_c \rightarrow \pm\infty} U_{\text{NL}}(\phi_c)/|\phi_c|^\gamma = 0$
- (2) Type 2 (superlinear [70]):  
 $\lim_{\phi_c \rightarrow \pm\infty} \phi_c^2/U_{\text{NL}}(\phi_c) = 0$
- (3) Type  $L$  (quasilinear):  
 $\exists \mathfrak{Q} > 0 : \lim_{\phi_c \rightarrow \pm\infty} U_{\text{NL}}(\phi_c)/\phi_c^2 = 1/2\mathfrak{Q}$  and  
 $U_{\text{NL}}(\phi_c) - \phi_c^2/2\mathfrak{Q}$  describes a type-1 inductor

Note that not all possible nonlinear inductors can be classified into one of the three types we provide. In Sec. III C, we discuss a nonlinear inductor whose potential does not have a well-defined leading term for large values of  $\phi_c$ . In Sec. III D, we provide an example for a nonlinear inductor with an asymmetric potential that is not of type 1(b).

As we show in the following, in the limit  $C'/C \rightarrow 0$ , the dynamics of the regular circuit shown in Fig. 4 strongly depends on which type of nonlinear inductor is considered. In particular, we prove the validity of a perturbative treatment in which, depending on the type of the nonlinear inductor in the circuit in Fig. 4, either the potential of the linear inductor or that of the nonlinear one can be identified

as the perturbation to the rest of the Hamiltonian. Finally, for each type of nonlinear inductor, we provide expressions for  $U_{\text{BO}}(\phi)$  in the limit of  $C'/C \rightarrow 0$ , and we associate an effective inductor with the Born-Oppenheimer potential in that limit.

### 1. Effective potential for sublinear inductors (type 1)

We start with the analysis of nonlinear inductors of type 1. In the following theorem, we show that for a nonlinear inductor of type 1(a), the Born-Oppenheimer potential vanishes as  $C'/C \rightarrow 0$ ; the nonlinear branch is replaced by an open circuit.

After presenting our formal results, we examine in Sec. IV the practical manifestations and consequences of this tendency to open-circuit behavior.

**Theorem 1.** Consider  $H_{\text{fast}}$  as defined in Eq. (16) with  $U_{\text{NL}}(\phi_c)$  describing a nonlinear inductor of type 1(a). Then,  $U_{\text{BO}}(\phi)$  as defined in Eq. (19) satisfies

$$\forall \phi \in \mathbb{R}: \lim_{C' \rightarrow 0} U_{\text{BO}}(\phi) = 0.$$

The general strategy of the proof, which we present in Appendix B 1, is as follows: While all the eigenvalues of  $H_{\text{fast}}$  in Eq. (16) diverge like  $1/\sqrt{C'}$  as  $C' \rightarrow 0$ , we note that if this diverging factor is scaled out, the Hamiltonian can be brought into the form of a standard harmonic oscillator plus an additional term that can be considered a perturbation for all potentials  $U_{\text{NL}}(\phi_c)$  of type 1(a). With the use of several auxiliary bounding Hamiltonians, we show that the results from analytic perturbation theory can be used [despite the fact that  $U_{\text{NL}}(\phi_c)$  may not be analytic in  $\phi_c$ ] to show that the resulting Rayleigh-Schrödinger series is well behaved and absolutely convergent. An evaluation of the appropriate terms in this series gives the result of the theorem.

One can lift the restriction that  $U_{\text{NL}}(\phi_c)$  is symmetric and also obtain a Born-Oppenheimer potential that vanishes in the limit  $C' \rightarrow 0$  if  $\lim_{\phi_c \rightarrow \pm\infty} U_{\text{NL}}(\phi_c)/|\phi_c|^\gamma = 0$  with  $\gamma \in (0, 1)$ , as the following theorem shows.

**Theorem 2.** Consider  $H_{\text{fast}}$  as defined in Eq. (16) with  $U_{\text{NL}}(\phi_c)$  describing a nonlinear inductor of type 1(b). Then,  $U_{\text{BO}}(\phi)$  as defined in Eq. (19) satisfies

$$\forall \phi \in \mathbb{R}: \lim_{C' \rightarrow 0} U_{\text{BO}}(\phi) = 0.$$

We refer to Appendix B 2 for a proof of Theorem 2.

Note that in this theorem the potential  $U_{\text{NL}}(\phi_c)$  need not be symmetric, i.e.,  $U_{\text{NL}}(\phi_c) \neq U_{\text{NL}}(-\phi_c)$ . Also, we note that nonlinear inductors of type 1(b) include the large class of nonlinear inductors that are described by a bounded potential, i.e.,  $|U_{\text{NL}}(\phi_c)| \leq M$  for all  $\phi_c$  and some  $M > 0$ . The Josephson junction, the superconducting quantum interference device (SQUID), and the SNAIL are probably the most important representatives of this class of inductors. For example, besides the SNAIL, Josephson junctions

with broken time-reversal symmetry are described by an asymmetric potential  $U_{\text{NL}}(\phi_c)$ ; see p. 414 in Ref. [71] and references therein.

To recap, within the framework of the Born-Oppenheimer approximation, which becomes more accurate the smaller the capacitance ratio  $C'/C$  is, we show that the inductive branch in the circuit in Fig. 4, i.e., the series combination of the linear inductance and the generic nonlinear inductor of type 1 (including its intrinsic capacitance), effectively becomes an open circuit as  $C'/C \rightarrow 0$ .

### 2. Effective potential for superlinear inductors (type 2)

Next, we consider the Born-Oppenheimer potential for nonlinear inductors of type 2. Here, we focus on nonlinear inductors of type 2 that are described by the following infinite set of potentials:

$$U_{\text{NL}}(\phi_c) = \beta |\phi_c|^\gamma, \quad \beta > 0, \quad \gamma \in \mathbb{Q}^{>2}. \quad (20)$$

In the following, we show that for a nonlinear inductor of type 2 with a potential of the form of Eq. (20), the Born-Oppenheimer potential approaches the potential of the linear inductance  $L$  as  $C'/C \rightarrow 0$ . Thus, in this limit, the nonlinear branch is replaced by a short circuit, meaning that one sets  $\phi_c = 0$ . To show this, our strategy is to identify the contribution of the linear inductance  $L$  in the fast Schrödinger equation in Eq. (17) as a perturbation, the opposite of the type-1 scenario. To this end, we provide the following theorem.

**Theorem 3.** Consider  $H_{\text{fast}}$  as defined in Eq. (16) with  $U_{\text{NL}}(\phi_c)$  as defined in Eq. (20) describing a subset of nonlinear inductors of type 2. Then,  $U_{\text{BO}}(\phi)$  as defined in Eq. (19) satisfies

$$\forall \phi \in \mathbb{R}: \lim_{C' \rightarrow 0} U_{\text{BO}}(\phi) = \frac{\phi^2}{2L}.$$

The proof of Theorem 3 is presented in Appendix B 3. At this point, we do not attempt to provide a general proof, but we conjecture that Theorem 3 holds for any generic nonlinear inductor of type 2 and is not restricted to potentials of the form of Eq. (20).

### 3. Effective potential for quasilinear inductors (type L)

Next, we analyze nonlinear inductors of type  $L$ . Note that an inductor of type  $L$  is not in general linear, but it is clear from the definition that its potential is the sum of that of a linear inductance  $\mathfrak{L}$  with that of a nonlinear inductor, with a potential  $U_{\text{NL}}(\phi_c) - \phi_c^2/2\mathfrak{L}$  that is of type 1. In other words, the type- $L$  inductor can always be represented as the parallel combination of a linear inductance and a nonlinear inductor of type 1. This equivalence will be useful later.

In the following, we show that for a nonlinear inductor of type  $L$ , the Born-Oppenheimer potential approaches the potential of a total linear inductance  $L + \mathfrak{L}$  as  $C'/C \rightarrow 0$ . Thus, in this limit, the nonlinear branch is replaced by a

linear inductance  $\mathfrak{L}$ , and the node  $\phi_c$  is removed by adding the linear inductances  $L$  and  $\mathfrak{L}$  in a series connection, resulting in a total inductance  $L + \mathfrak{L}$  between the nodes  $\phi$  and ground. This analysis results in the following theorem.

**Theorem 4.** Consider  $H_{\text{fast}}$  as defined in Eq. (16) with  $U_{\text{NL}}(\phi_c)$  describing a nonlinear inductor of type  $L$ . Then,  $U_{\text{BO}}(\phi)$  as defined in Eq. (19) satisfies

$$\forall \phi \in \mathbb{R}: \lim_{c \rightarrow 0} U_{\text{BO}}(\phi) = \frac{\phi^2}{2(L + \mathfrak{L})}$$

with  $\mathfrak{L} = \lim_{\phi_c \rightarrow \infty} \phi_c^2 / 2U_{\text{NL}}(\phi_c) > 0$ .

We prove Theorem 4 in Appendix B 4.

### C. A pathological potential

Not all series combinations of a linear inductance and a nonlinear inductor (cf. Fig. 4) necessarily have a well-defined effective limiting behavior as the internal capacitance vanishes. To illustrate the potentially ambiguous limit, we analyze a pathological example of a nonlinear inductor with a potential energy that cannot be classified as falling into one of our categories.

First, we focus on an isolated nonlinear inductor accompanied by its internal shunting capacitance. Working with dimensionless variables, the Hamiltonian of this system can be written as

$$H = \frac{p_y^2}{2m} + U_{\text{NL}}(y), \quad (21)$$

in which  $m$  denotes the rescaled shunting capacitance. The rescaled canonical variables satisfy the dimensionless commutation relation  $[y, p_y] = i$ . In the following, we consider a nonlinear inductor that is described by the following symmetric, differentiable potential ( $n \in \mathbb{Z}$ ):

$$U_{\text{NL}}(y) = \begin{cases} 10^{(3-4n+2\log_{10}|y|)^3+8n-7}y^{-2} & \text{for } 10^{2n-2} \leq |y| \leq 10^{2n-1} \\ 10^{-4n}y^4 & \text{for } 10^{2n-1} \leq |y| \leq 10^{2n}. \end{cases} \quad (22)$$

The potential  $U_{\text{NL}}(y)$  and the corresponding ground-state wave function of the Hamiltonian in Eq. (21) for different values of  $m$  are shown in Fig. 5. Because of the self-similarity of the potential

$$U_{\text{NL}}(10^2 y) = 10^4 U_{\text{NL}}(y), \quad (23)$$

the eigensystem of  $H$  associated with the mass  $m$  relates to that with a rescaled mass  $m' = 10^{-8}m$ . In that case, the eigenenergies and the eigenstates satisfy  $E'_\nu = 10^4 E_\nu$  and  $\psi'_\nu(y) \propto \psi_\nu(y/100)$ , respectively.

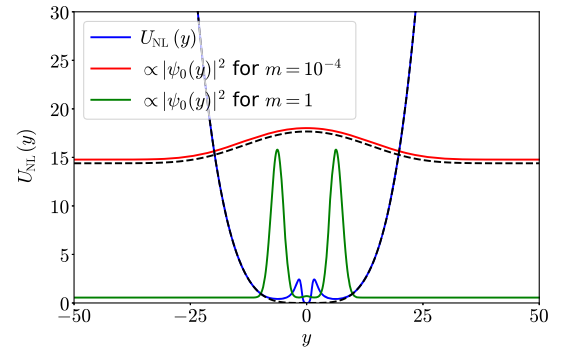


FIG. 5. Pathological potential  $U_{\text{NL}}(y)$  in Eq. (22) (blue) together with the ground-state wave function of the Hamiltonian in Eq. (21) for  $m = 10^{-4}$  (red) and  $m = 1$  (green). Different choices of  $m$  correspond to different values of the internal shunting capacitance. For  $m = 10^{-4}$ , the ground-state wave function of the potential  $y^4/10^4$  is shown for comparison (black dashed lines for both wave function and potential). For better visibility, all wave functions are scaled by a factor 10 and shifted by their corresponding ground-state energies.

We partition the range of  $m$  into three distinct regions in which the eigensystem of  $H$  behaves qualitatively differently; see also Fig. 6. First, there is a region of  $m$  in which both the ground-state energy and the ground-state wave function are well approximated by that of a purely quartic potential  $\propto y^4$  (red wave function in Fig. 5). Second, there is a disjoint region of  $m$  in which the ground-state wave function resembles that of a double-well potential (green wave function in Fig. 5). Within these two regions, the scaling of, e.g., the eigenenergies with respect to  $m$ , is fundamentally different. Last, there are intermediate values of  $m$  in which the system transitions between both the previously mentioned regions. Thus, by construction of  $U_{\text{NL}}(y)$ , there is no well-defined asymptotic behavior of the eigensystem as  $m \rightarrow 0$ .

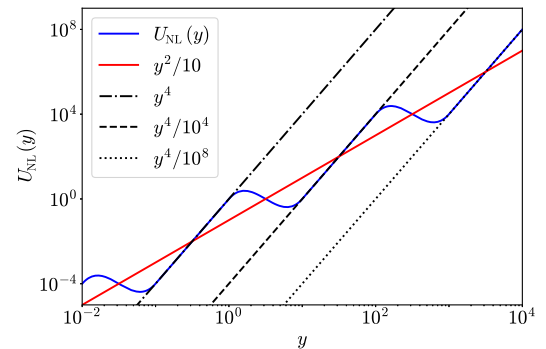


FIG. 6. Pathological potential  $U_{\text{NL}}(y)$  in Eq. (22) (blue) together with the global trend  $y^2/10$  (red). For  $|y| \in [10^{2n-1}, 10^{2n}]$  with  $n \in \mathbb{Z}$ ,  $U_{\text{NL}}(y)$  grows faster than a second-order polynomial, in particular,  $U_{\text{NL}}(y) \propto y^4$  (indicated with black lines). However, in the limit  $y \rightarrow \infty$ , the ratio  $U_{\text{NL}}(y)/y^2$  remains ill-defined.

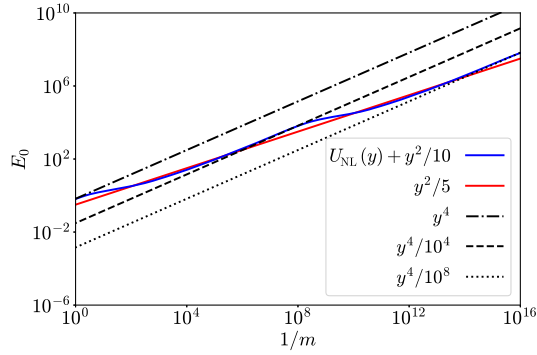


FIG. 7. Ground-state energy  $E_0$  of  $H_{\text{fast}}$  in Eq. (25) for a fixed value  $x = 0$  as a function of  $1/m$  (blue). For certain regimes of  $m$ ,  $E_0$  is well approximated by the ground-state energy corresponding to a purely quartic potential (indicated with black lines). On large scales of  $m$ , however,  $E_0$  follows the global trend of the ground-state energy corresponding to a purely quadratic potential (red).

Next, we embed such a nonlinear inductor in the circuit shown in Fig. 4. We choose the linear inductance such that the total system is described by the Hamiltonian [cf. Eq. (15)]

$$H_r = \frac{p_x^2}{2M} + \frac{p_y^2}{2m} + U_{\text{NL}}(y) + \frac{(y-x)^2}{10}, \quad (24)$$

in which  $M$  is the rescaled outer capacitance, and  $x$  and  $y$  can be interpreted as slow and fast variables, respectively. The ground-state energy  $E_0$  of the fast part of  $H_r$  [cf. Eq. (16)]

$$H_{\text{fast}} = \frac{p_y^2}{2m} + U_{\text{NL}}(y) + \frac{(y-x)^2}{10} \quad (25)$$

is shown in Fig. 7 for  $x = 0$ . For the special choice  $x = 0$ , the total potential entering  $H_{\text{fast}}$  remains self-similar in  $y$ . As a consequence,  $E_0$  scales linearly by  $10^4$  as  $1/m$  is scaled by a factor  $10^8$ . For certain regimes of  $m$ , the ground-state energy is well approximated by that of a bare quartic potential; see black lines in Fig. 7. However, if the mass  $m$  is considered over several orders of magnitude,  $E_0$  follows the “global trend” given by the ground-state energy corresponding to that of a quadratic potential; see red line in Fig. 7.

For fixed values of  $m$ , we use the ground-state energy of  $H_{\text{fast}}$  at  $x = 0$  to shift the Born-Oppenheimer potential such that  $U_{\text{BO}}(0) = 0$ . The Born-Oppenheimer potential  $U_{\text{BO}}(x)$  for the specific choice  $x = 10$  is shown in Fig. 8 as a function of  $1/m$ . As before, we note that for certain regimes of  $m$ , the Born-Oppenheimer potential associated with  $U_{\text{NL}}(y)$  in Eq. (22) is well approximated by that corresponding to a nonlinear inductor that is described by a purely quartic potential  $\propto y^4$ ; see black curves in Fig. 8. In fact, recall that for nonlinear inductors of type 2 (to which

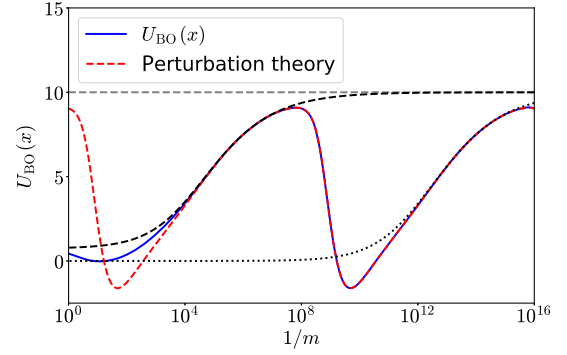


FIG. 8. Born-Oppenheimer potential  $U_{\text{BO}}(x)$  evaluated at  $x = 10$  as a function of  $1/m$  (blue). The red dashed line showing the result of the second-order perturbation theory in  $x$  is periodic in  $\log(1/m)$ ; see main text. For nonlinear inductors of type 2,  $U_{\text{BO}}(10)$  approaches the value of 10 in the limit of  $m \rightarrow 0$  (gray dashed line). For comparison, black lines show the Born-Oppenheimer potential at  $x = 10$  with a nonlinear inductor that is described by a purely quartic potential (dashed,  $y^4/10^4$ ; dotted,  $y^4/10^8$ ).

quartic potentials belong) the Born-Oppenheimer potential approaches the value of  $x^2/10$  (cf. Theorem 3) in the limit of  $m \rightarrow 0$ . However, such a convergence is not observed for  $U_{\text{BO}}(x)$  involving  $U_{\text{NL}}(y)$  in Eq. (22) as this potential does not describe a nonlinear inductor of type 2. In order to analyze the behavior of  $U_{\text{BO}}(x)$  for small values of  $m$ , we note that  $H_{\text{fast}}$  in Eq. (25) corresponding to  $m$  and  $x$  relates to that corresponding to  $m' = 10^{-8}m$  and  $x' = 10^2x$ . In particular, we find that  $H'_{\text{fast}} = 10^4 H_{\text{fast}}$ . As a consequence, for small enough values of  $m$ , nonzero values of  $x$  can be incorporated with second-order perturbation theory (red dashed line in Fig. 8), which in fact becomes more precise as  $m$  becomes smaller. As a result, we find that (up to small corrections)  $U_{\text{BO}}(x)$  is periodic in  $\log(1/m)$  for small values of  $m$ .

In total, the nonlinear inductor described by the pathological potential in Eq. (22) exemplifies that not every series combination of inductances gives rise to a well-defined single effective inductance as the internal capacitance vanishes. In particular, we conclude that if one cannot classify a nonlinear inductor at hand by means of the results presented in Secs. III B 1–III B 3, then one is required to know the particular value of its internal capacitance in order to derive a reliable one-mode replacement.

#### D. An asymmetric potential

The following shows that the result of Theorem 2 is tight: The Born-Oppenheimer potential does not vanish for a linear, asymmetric inductive potential. We provide the Born-Oppenheimer analysis for this simple asymmetric example: We consider the piecewise linear potential

$$U_{\text{NL}}(\phi_c) = b[1 + a\Theta(\phi_c)]|\phi_c|, \quad b > 0, \quad (26)$$

in which  $a > 0$  tunes the asymmetry. Here,  $b$  is some arbitrary positive prefactor, and  $\Theta(\phi_c)$  denotes the Heaviside step function. Despite the asymmetry of  $U_{\text{NL}}(\phi_c)$ , the fact that  $\lim_{\phi_c \rightarrow \pm\infty} U_{\text{NL}}(\phi_c)/\phi_c^2 = 0$  allows the Born-Oppenheimer potential following the steps in the proof of Theorem 1 (cf. Sec. III B 1). In particular, recall that the zero-point fluctuation  $\Phi_{\text{ZPF}}$  as defined in Eq. (B2) diverges as the intrinsic capacitance  $C'$  vanishes. Thus, we proceed by treating  $U_{\text{NL}}(\phi_c)$  in Eq. (26) as part of a perturbation around the harmonic-oscillator Hamiltonian; expanding the Born-Oppenheimer potential in powers of  $1/\Phi_{\text{ZPF}}$  yields

$$U_{\text{BO}}(\phi) = \frac{ab\phi}{2} + \frac{(2+a)b\phi^2 - a(2+a)b^2L\phi}{2\sqrt{\pi}\Phi_{\text{ZPF}}}, \quad (27)$$

where we omit terms of the order  $\mathcal{O}(1/\Phi_{\text{ZPF}}^2)$ . We observe that  $U_{\text{BO}}(\phi)$  does not vanish as  $1/\Phi_{\text{ZPF}} \rightarrow 0$  if the asymmetric case  $a \neq 0$  is considered. To interpret this result, we rewrite  $U_{\text{BO}}(\phi)$  in Eq. (27) in normal form,

$$U_{\text{BO}}(\phi) = \frac{(2+a)b}{2\sqrt{\pi}\Phi_{\text{ZPF}}} \left[ \phi + \frac{a}{2} \left( \frac{\sqrt{\pi}\Phi_{\text{ZPF}}}{2+a} - bL \right) \right]^2, \quad (28)$$

in which we drop an additive constant that does not depend on  $\phi$ . Thus, if no further network element besides the shunting capacitance  $C$  is attached to the node flux  $\phi$  (see Fig. 4), the slow degree of freedom of the system is well approximated by  $H_{r,\text{eff}}$  in Eq. (18), and its ground-state wave function is a Gaussian whose center position and standard deviation are given by

$$\phi_m = -\frac{a}{2} \left( \frac{\sqrt{\pi}\Phi_{\text{ZPF}}}{2+a} - bL \right), \quad \Delta\phi = \sqrt{\hbar}^4 \sqrt{\frac{\sqrt{\pi}\Phi_{\text{ZPF}}}{(2+a)bC}}, \quad (29)$$

respectively. In the limit of large zero-point fluctuations, we find that  $\Delta\phi/\phi_m \rightarrow 0$ , while  $\Delta\phi \rightarrow \infty$ . Thus, when capacitively shunted, the series combination of a linear inductance and our nonsymmetric, nonlinear inductor is effectively replaced by an open circuit, as in the case of a nonlinear inductor of type 1. However, if the node  $\phi$  is embedded into a larger circuit, the displacement  $\phi_m$  has the effect of an effective magnetic flux through a closed loop formed by the inductive branch and further inductive elements. This effective magnetic flux does not affect the dynamics of the total system as long as the larger circuit involves linear inductances only. If, however, the system contains further nonlinear inductors, the actual value of  $\phi_m$  and thus that of the small intrinsic capacitance  $C'$  becomes of central importance. In that case, an effective replacement of the inductive branch in the circuit in Fig. 4 is not well defined as the internal capacitance  $C'$  vanishes.

## IV. JOSEPHSON-JUNCTION DEVICES

We turn now to applications. The primary nonlinear inductance available in the lab is, of course, the Josephson junction. But from this specific nonlinearity a wide variety of effective inductances are built, for specific novel characteristics in fluxonium [22] and the  $0-\pi$  qubit [10,11,72], for emergent linear devices (superinductors [73]) with large effective  $L$  value, and for optimal couplers and amplifier structures [74,75]. Many workers view these complex devices as key to fundamentally improving the superconducting qubit [20,76–78].

Even the original flux qubit [79,80] was thought of as a realization of our simple circuit Fig. 3(a) with the linear inductor being approximately realized by a series combination of two large- $E_J$  junctions. This original work avoided any singular treatment, but subsequent work has not always been so careful.

The Josephson junction has an additional feature that we do not treat above, namely, that its potential characteristic is periodic. This has the consequence that the flux variable  $\phi$  can be treated as compact on the domain  $(0, \Phi_0]$ , leading also to the charge on the nodes of the junction being constrained by the uncertainty relationship  $\Delta\phi\Delta Q \approx \hbar$  (see Secs. 2B and 5.10 of Ref. [81]). Thus, the tendency identified in our analysis of  $\Delta\phi$  to diverge as  $C'$  becomes small is associated with the emergence of a definite value of the node charge. This is precisely the phenomenon of the Coulomb blockade [82]. The Coulomb blockade has been known, in experiments long predating the emergence of qubits, to be associated with the occurrence of a superconducting-insulating transition [83]. The open-circuit behavior that we obtain above is a few-body version of this many-body phase transition.

The need to avoid this fluctuation-dominated, insulating regime was recognized in one of the first proposals for a protected qubit, the current-mirror qubit [10,72]. In its simplified version, the  $0-\pi$  qubit, it was recognized [11] that the desired superinductor should operate at very high impedance value, which has been approached only very gradually in subsequent experiments [15].

To link these active areas of work to our formalism, we now provide a full Born-Oppenheimer analysis of one of the simpler multijunction structures in current use, the SNAIL.

### A. Josephson-junction arrays: Single-phase approximation revised

So far, we analyzed a series connection of a linear inductance and a nonlinear inductor. In this section, we generalize this analysis, and we consider the series connection of multiple nonlinear inductors. This is important because, as we have just discussed, arrays of Josephson junctions are commonly fabricated to realize effective devices such as superinductances [11,22,23] or SNAILS [27–29]. Therefore, in the following, we revise the

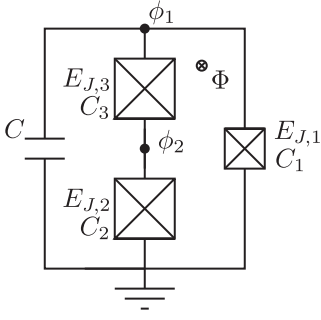


FIG. 9. Capacitively-shunted SNAIL with  $N = 2$  large Josephson junctions. The external magnetic flux  $\Phi$  pierces the loop formed by the Josephson junctions.

single-phase approximation [84] that is commonly used to simplify the description of these multinode Josephson-junction chains. Here, we focus our analysis on the case of a capacitively-shunted SNAIL with  $N = 2$  large Josephson junctions [85]; see Fig. 9.

Typically, SNAILs are embedded into larger electrical networks in order to provide nonlinearity in the form of effective nonlinear inductors, or for the amplification of signals. In any case, the internal degrees of freedom of the SNAIL (here  $\phi_2$ ) are commonly discarded such that it can be considered to be an element of 1 degree of freedom only (here  $\phi_1$ ). This simplification is known as the single-phase approximation.

We introduce the dimensionless parameters  $k_i = C_i/C$  that relate the intrinsic capacitances  $C_i$  of the Josephson junctions to the large capacitance  $C$  of the shunt. In the following model, we consider all the intrinsic capacitances of the Josephson junctions to be finite, i.e.,  $k_i > 0$ . As a consequence, every branch of a SNAIL network, such as shown in Fig. 9, contains at least one capacitor, and the capacitance matrix

$$\mathbf{C} = \begin{pmatrix} 1 + k_1 + k_3 & -k_3 \\ -k_3 & k_2 + k_3 \end{pmatrix} \quad (30)$$

is invertible. Thus, the circuit is regular, and the corresponding Hamiltonian is straightforwardly obtained as

$$H = 4E_C \mathbf{n}^T \mathbf{C}^{-1} \mathbf{n} + U(\boldsymbol{\phi}) \quad (31)$$

with the charging energy  $E_C = e^2/2C$ , and the vector notation is  $\boldsymbol{\phi} = (\phi_1, \phi_2)^T$ ,  $\mathbf{n} = (n_1, n_2)^T$ . The Josephson junctions constitute the total potential energy

$$U(\boldsymbol{\phi}) = -E_{J,1} \cos(\phi_1) - E_{J,2} \cos(\phi_2) - E_{J,3} \cos(\phi_1 - \phi_2 + \Phi), \quad (32)$$

in which  $\Phi = \Phi^{\text{ext}}/\Phi_0$  is the rescaled external magnetic flux through the loop formed by the Josephson junctions. Similarly, the chosen variables  $\phi_i$  and  $n_j$  are dimensionless,

and the system is quantized by imposing the usual commutation relations  $[\phi_i, n_j] = i\delta_{ij}$ .

In order to proceed, we diagonalize the kinetic term of the Hamiltonian in Eq. (31). As we see, in the limit of small intrinsic capacitances ( $k_i \ll 1$ ), this diagonalization clearly separates the dynamics of the system into a fast variable and a slow one. In principle, such a decoupling can be achieved by means of several different variable transformations. Here, we define the canonical (but nonorthogonal) variable transformation obtained from a Cholesky decomposition:

$$\mathbf{p} = \mathbf{A}^{-1} \mathbf{n}, \quad \mathbf{x} = \mathbf{A}^T \boldsymbol{\phi}, \quad \mathbf{A} = \begin{pmatrix} 1 & -k_3 \\ 0 & k_2 + k_3 \end{pmatrix}, \quad (33)$$

which transforms the Hamiltonian of the system to

$$H = 4E_C (d_1 p_1^2 + d_2 p_2^2) + U(x_1, x_2) \quad (34)$$

with the diagonal kinetic matrix elements

$$d_1 = \frac{k_2 + k_3}{k_2 + k_3 + k_1 k_2 + k_2 k_3 + k_3 k_1}, \quad d_2 = \frac{1}{k_2 + k_3}, \quad (35)$$

and the total potential energy  $U(x_1, x_2)$  in terms of the new positionlike variables  $x_1$  and  $x_2$ ,

$$U(x_1, x_2) = -E_{J,1} \cos(x_1) - E_{J,2} \cos\left(\frac{k_3}{k_2 + k_3} x_1 + x_2\right) - E_{J,3} \cos\left(\frac{k_2}{k_2 + k_3} x_1 - x_2 + \Phi\right). \quad (36)$$

Note that, per construction, the variable transformation in Eq. (33) ensures that  $[x_i, p_j] = i\delta_{ij}$  and  $x_1 = \phi_1$ . The latter property will be crucial for the single-phase approximation of the SNAIL if it is coupled inductively to some further circuitry, as the relevant coupling variable will be  $\phi_1$  in that case. The effect of the nonorthogonal transformation matrix  $\mathbf{A}$  on the boundary conditions of the wave function is discussed in Sec. IV A 3.

In the following, we analyze the limit of small intrinsic capacitances, i.e.,  $k_i \ll 1$ . In that limit, we find that  $d_2 \gg d_1$  such that the dynamics in the  $x_2$  direction becomes much faster than that in the  $x_1$  direction. As we elaborate in Sec. III, such different timescales for the dynamics in the two directions make the Born-Oppenheimer approximation applicable. Thus, we first solve the Schrödinger equation for the fast variable  $x_2$ , keeping the slow variable  $x_1$  as a fixed parameter. To further simplify the analysis, the following calculations are carried out for a symmetric SNAIL; i.e., for the remainder of this section, we focus on the special case of  $k_2 = k_3$  and  $E_{J,2} = E_{J,3}$ .

### 1. Classical approach

Instead of solving the fast Schrödinger equation for its quantum-mechanical ground-state energy, it has been typical to focus on the classical minimal energy of  $U(x_1, x_2)$  in the  $x_2$  direction for fixed values of  $x_1$  [28,84]. As we illustrate in Sec. II, this simplification corresponds to the singular case ( $k_2 = 0$ ), in which quantum fluctuations in  $\phi_2$  are assumed to be absent, and the Dirac-Bergmann algorithm has to be applied in order to obtain the Hamiltonian. However, for the regular case ( $k_2 > 0$ ), this classical approach is a good approximation only if the eigenfunction is well localized in  $x_2$ , which is true if all the individual Josephson junctions in the array are deeply in the transmon regime,  $E_C/k_2E_{J,2} \ll 1$  [86]. Note that these two conditions on  $k_2$  are not automatically compatible and need to be examined individually for each given set of circuit parameters; see also Appendix A in Ref. [28].

For the symmetric SNAIL and a fixed value of  $x_1$ , the condition for a minimal potential [Eq. (36)] in the fast direction evaluates to  $x_2 = \Phi/2$ . Inserting this value for  $x_2$  in  $U(x_1, x_2)$  results in an effective one-dimensional potential for the slow  $x_1$  variable, namely,

$$U_{\text{BO}}^{\text{cl}}(x_1) = -E_{J,1} \cos(x_1) - 2E_{J,2} \cos\left(\frac{x_1 + \Phi}{2}\right). \quad (37)$$

This classically obtained Born-Oppenheimer potential is known as the single-phase approximation and simplifies the circuit in Fig. 9 as it discards the dynamics of the slow internal degree of freedom. However, note that  $U(x_1, x_2)$  is minimal in the fast direction at  $x_2 = \Phi/2$  only if  $|x_1 + \Phi| < \pi$  (discarding the periodicity). In particular, for  $x_1 = \pi - \Phi$ , we find that  $U(\pi - \Phi, x_2)$  does not depend on  $x_2$ , and thus,  $x_2$  is not unambiguously a fast variable compared to  $x_1$ , which might have consequences for the validity of the Born-Oppenheimer approximation. For this reason, one must also require the wave function in  $x_1$  to be localized “far enough away” from these critical points. Keeping this potential breakdown of the Born-Oppenheimer approximation in mind, we proceed with the analysis of finite but small quantum fluctuations in the fast variable  $x_2$ .

### 2. Harmonic oscillator approach

In order to obtain a more accurate approximation for the Born-Oppenheimer potential than that in Eq. (37), we expand the potential  $U(x_1, x_2)$  up to second order in  $x_2$  around its minimum in the fast direction,

$$U(x_1, x_2) = U_{\text{BO}}^{\text{cl}}(x_1) + E_{J,2} \cos\left(\frac{x_1 + \Phi}{2}\right) \left(x_2 - \frac{\Phi}{2}\right)^2, \quad (38)$$

and we omit terms of the order  $\mathcal{O}[(x_2 - \Phi/2)^3]$ . Then, the ground-state energy of the resulting harmonic oscillator in the  $x_2$  direction is taken to define the effective Born-Oppenheimer potential for  $x_1$ ,

$$U_{\text{BO}}^{\text{HO}}(x_1) = U_{\text{BO}}^{\text{cl}}(x_1) + \sqrt{\frac{2}{k_2} E_C E_{J,2}} \cos\left(\frac{x_1 + \Phi}{2}\right). \quad (39)$$

As in the purely classical approach, the harmonic approximation is valid only if the wave function is well localized in  $x_2$ , i.e., if  $E_C/k_2E_{J,2} \ll 1$  (the transmon limit mentioned above). Also, we again require  $|x_1 + \Phi| < \pi$  (discarding the periodicity) in order to expand around an actual minimum and not around a maximum. Equation (39) already improves the classical Born-Oppenheimer potential as the additional correction term takes account of the zero-point energy due to finite quantum fluctuations.

The result for  $U_{\text{BO}}^{\text{HO}}(x_1)$  can be used to improve the classical Born-Oppenheimer potential by renormalizing the Josephson energy  $E_{J,2}$  instead of adding a correction term [87]. To this end, we note that the second-order Maclaurin polynomial of both the functions  $2\sqrt{\cos(\epsilon)}$  and  $\cos(\epsilon) + 1$  coincides. Therefore, after dropping a constant shift in energy, we approximate  $U_{\text{BO}}^{\text{HO}}(x_1)$  as

$$U_{\text{BO}}^{\text{HO}}(x_1) \approx U_{\text{BO}}^{\text{cl}}(x_1) + \sqrt{\frac{1}{2k_2} E_C E_{J,2}} \cos\left(\frac{x_1 + \Phi}{2}\right). \quad (40)$$

Finally, this approximation is used to identify the renormalized Josephson energy

$$\tilde{E}_{J,2} = E_{J,2} \left(1 - \frac{1}{2} \sqrt{\frac{1}{2k_2} \frac{E_C}{E_{J,2}}}\right) \quad (41)$$

such that  $U_{\text{BO}}^{\text{HO}}(x_1) \approx \tilde{U}^{\text{cl}}(x_1)$  with

$$\tilde{U}_{\text{BO}}^{\text{cl}}(x_1) = -E_{J,1} \cos(x_1) - 2\tilde{E}_{J,2} \cos\left(\frac{x_1 + \Phi}{2}\right). \quad (42)$$

We conclude the analysis of small finite quantum fluctuations of the internal degrees of freedom in the SNAIL with the remark that a similar renormalization of the Josephson energy was reported in Ref. [89]. There, an effective single-mode theory for the fluxonium qubit is derived that incorporates possible capacitances to ground as well as disorder in the circuit elements. Specializing to a symmetric SNAIL with  $N = 2$  Josephson junctions in the array, the reported renormalization coincides with Eq. (41) up to leading order in  $\sqrt{E_C/k_2E_{J,2}} \ll 1$ .

Nevertheless, we see that other current analyses, even those specifically set up to understand the effect of capacitive effects in array structures as in fluxonium [23], do not fully account for the  $E_J$  renormalization effect.

In any of the many current structures in which inductive structures are built from Josephson arrays, these renormalization effects must be evaluated.

### 3. Limit of small internal capacitances

Both the Born-Oppenheimer potential based on the classical minimal energy (Sec. IV A 1) and that based on the harmonic-oscillator approximation (Sec. IV A 2) require the wave function to be localized at or close to the minimum in the fast  $x_2$  direction, respectively. As discussed, this requirement is fulfilled if  $E_C/k_2E_{J,2} \ll 1$ . For intermediate values  $E_C/k_2E_{J,2} \simeq 1$ , quantum fluctuations in  $x_2$  are too large to allow for a quadratic expansion of the potential. In that case, one must solve the fast part of the Schrödinger equation numerically or attempt to find an (approximate) analytic solution. However, for vanishingly small but finite internal capacitances  $E_C/k_2E_{J,2} \gg 1$ , quantum fluctuations in  $x_2$  dominate the eigenenergies of the fast Schrödinger equation. In the following, we compare this limit with the singular case ( $k_2 = 0$ ) according to the Dirac-Bergmann algorithm. We expect the wave function to be widely extended, and therefore we first analyze its boundary conditions. Given the initial flux variables  $\phi_1$  and  $\phi_2$ , the boundary conditions on the full two-dimensional wave function  $\Psi(\phi_1, \phi_2)$  read [90]

$$\Psi(\phi_1 + 2\pi, \phi_2) = e^{i2\pi\nu_1}\Psi(\phi_1, \phi_2), \quad (43a)$$

$$\Psi(\phi_1, \phi_2 + 2\pi) = e^{i2\pi\nu_2}\Psi(\phi_1, \phi_2). \quad (43b)$$

Here,  $\nu_1$  and  $\nu_2$  take account of possible offset charges on the superconducting islands of the network in Fig. 9. However, we want to evaluate the wave function in the  $x_1$ - $x_2$  representation, and the nonorthogonal variable transformation in Eq. (33) imposes “spiral” boundary conditions on  $\Psi(x_1, x_2)$ , namely,

$$\Psi(x_1 + 2\pi, x_2 - \pi) = e^{i2\pi\nu_1}\Psi(x_1, x_2), \quad (44a)$$

$$\Psi(x_1, x_2 + 2\pi) = e^{i2\pi\nu_2}\Psi(x_1, x_2). \quad (44b)$$

The Born-Oppenheimer approximation assumes that the total wave function factorizes

$$\Psi(x_1, x_2) = \chi(x_1)\psi_{x_1}(x_2), \quad (45)$$

where the individual factors describe the fast and the slow degree of freedom, respectively. In particular,  $\psi_{x_1}(x_2)$  solves the fast part of the Schrödinger equation in which  $x_1$  is treated as a fixed parameter. The resulting eigenenergy—the Born-Oppenheimer potential—is then used as the potential for the effective slow part of the Schrödinger equation, which is solved by  $\chi(x_1)$ .

In the limit of vanishingly small internal capacitances, a convenient basis for solving the fast Schrödinger equation is set up by the plane waves

$$u_n(x_2) = \frac{1}{\sqrt{2\pi}} e^{i(\nu_2+n)x_2}, \quad n \in \mathbb{Z}, \quad (46)$$

as they comply with the boundary conditions in Eq. (44) and already diagonalize the kinetic term of the fast Hamiltonian,

$$\langle u_m | 4E_C d_2 p_2^2 | u_n \rangle = 4E_C d_2 (\nu_2 + n)^2 \delta_{m,n}. \quad (47)$$

Furthermore, the potential energy  $U(x_1, x_2)$  is tridiagonal in that basis. In particular, using the notation  $U_{m,n}(x_1) = \langle u_m | U(x_1, x_2) | u_n \rangle$ , we find that

$$U_{n,n}(x_1) = -E_{J,1} \cos(x_1), \quad (48a)$$

$$U_{n,n\pm 1}(x_1) = -\frac{E_{J,2}}{2} (e^{\mp ix_1/2} + e^{\pm ix_1/2} e^{\pm i\Phi}), \quad (48b)$$

while all the other matrix elements vanish.

For simplicity, in the following analysis we focus on the case  $\nu_2 = 0$ . Then, in the limit of vanishingly small internal capacitances,  $u_0(x_2)$  is a good approximation of the ground state of the fast Hamiltonian. In particular, in first-order perturbation theory, the resulting Born-Oppenheimer potential for the slow  $x_1$  variable

$$U_{\text{BO}}(x_1) = E_{J,1} [1 - \cos(x_1)] \quad (49)$$

is essentially that of the Josephson junction shunting the Josephson-junction array; see Fig. 9. Thus, we conclude that in the limit of vanishingly small intrinsic capacitances in the Josephson-junction array, the entire branch comprising it can be efficiently modeled as an open circuit. We see that this is similar to the case of a type-I inductor in series with a linear inductance; see Sec. III B 1.

Also, the kinetic term corresponding to the  $x_1$  variable, i.e., the  $\phi_1$ -node shunting capacitance, is in agreement with this result. In particular, in the limit of small  $k_2, k_3$ , we find

$$d_1 E_C \approx (1/E_C + 1/E_{C,1})^{-1}, \quad (50)$$

which is the effective charging energy of the parallel connection of  $C$  and  $C_1$ . This again coincides with the interpretation of the central branch in the circuit in Fig. 9 being absent.

## V. CONCLUSION AND OUTLOOK

Taking a final look at the fixed-point structure that our work uncovers, we offer a schematic “flow diagram” in Fig. 10. We of course do not use the tools of renormalization-group theory here, but flows are well defined in our work, obtained implicitly from the calculation of ground-state energies of fast-variable Hamiltonians in the Born-Oppenheimer treatment. While these flows are in a function space (i.e., infinite dimensional), they can usefully be schematized in the two-dimensional space shown.



To conclude, our work highlights the importance of critically examining the validity of well-tried theorems or simplifications from classical network synthesis, which build on Kirchhoff's conservation laws (e.g., the  $Y$ - $\Delta$  transformation or Tellegen's replacement rules for terminated gyrators [58,96]), prior to applying circuit quantization. We can envision our work to provide the basis for the quantization of unconventional electrical networks yet to be designed that, e.g., involve nonreciprocal elements or more general nonlinear elements going beyond the Josephson junction. Encouraged by the continuous progress in fabricating novel network elements such as on-chip nonreciprocal devices [97–101], nonlinear kinetic inductances [102,103], or nonlinear quantum capacitances [92–94], continuing development of the theoretical description of electrical networks containing such elements is highly motivated by the vast new possibilities they offer. Perhaps, someday, superconducting qubits with a nonlinear capacitor [104,105] or intrinsically protected qubits based on the nonreciprocity of the device [88] might open new, exciting pathways to the realization of a large-scale quantum processor.

### ACKNOWLEDGMENTS

We are most grateful to our colleague Fabian Hassler for many important suggestions and impulses at the early stages of the work reported here, as well as for suggesting the use of Youla's decomposition to effectively represent antisymmetric matrices. We thank Daniele Tampieri of TTlabs for insightful observations about convergence criteria for series. We thank Barry Simon for pointing out Ref. [106]. Thanks also to Alex Altland for observing the resemblance of the present work to the renormalization-group analysis of Kane and Fisher. We acknowledge support from the Deutsche Forschungsgemeinschaft (DFG, German Research Foundation) under Germany's Excellence Strategy—Cluster of Excellence Matter and Light for Quantum Computing (ML4Q) EXC 2004/1—390534769. D. D. V. gratefully acknowledges funding by the German Federal Ministry of Education and Research within the funding program “Photonic Research Germany” under Contract No. 13N14891, and within the funding program “Quantum Technologies—From Basic Research to the Market” (project GeQCoS), Contract No. 13N15685.

### APPENDIX A: AVOIDING THE BRANCHED HAMILTONIAN

In this appendix, we further analyze the singular Lagrangian

$$\mathcal{L} = \frac{m\dot{x}^2}{2} - \frac{(x-y)^2}{2} + \beta \cos(y), \quad (\text{A1})$$

which is a relabeled version of the Lagrangian in Eq. (9) describing the circuit in Fig. 3(a). As we elaborate in Sec. II B, after eliminating the variable  $y$  in the Lagrangian, the corresponding one-dimensional Hamiltonian  $H_s$  [see Eq. (12)] is branched if  $\beta > 1$ .

As opposed to this result, here we demonstrate that such a branched Hamiltonian can be avoided at the price of choosing different variables that are noncanonical. To this end, we apply the Dirac-Bergmann algorithm. The conjugate momenta  $p_x = \partial\mathcal{L}/\partial\dot{x}$ ,  $p_y = \partial\mathcal{L}/\partial\dot{y}$  give rise to one primary constraint

$$G_1 = p_y \simeq 0, \quad (\text{A2})$$

in which the weak equality sign  $\simeq$  reminds us that one must not use the equation before the Poisson brackets are evaluated. Accounting for this primary constraint via the Lagrange multiplier  $\mu$ , the primary Hamiltonian of the system reads

$$H_P = p_x\dot{x} + p_y\dot{y} - \mathcal{L} + \mu G_1, \quad (\text{A3})$$

and it governs the time evolution of the system. In particular, requiring that the time evolution of the primary constraint

$$\dot{G}_1 \simeq \{G_1, H_P\} \quad (\text{A4})$$

vanishes, results in a consistency condition that leads to the secondary constraint

$$G_2 = x - y - \beta \sin(y) \simeq 0, \quad (\text{A5})$$

which is essentially the Euler-Lagrange equation of motion for the  $y$  degree of freedom. Note that  $\dot{G}_2$  does not give rise to further constraints.

In the following, both the primary constraint and the secondary constraint are used to define the Dirac brackets—a redefinition of the Poisson brackets. To this end, we introduce the matrix

$$\mathbf{M} = \begin{pmatrix} 0 & \{G_1, G_2\} \\ \{G_2, G_1\} & 0 \end{pmatrix}, \quad (\text{A6})$$

which collects the mutual Poisson brackets of the constraints. In particular, we find

$$\{G_1, G_2\} = 1 + \beta \cos(y), \quad (\text{A7})$$

which, in general, does not vanish. Thus, both constraints  $G_1$  and  $G_2$  are second-class constraints. Next, Dirac's version of the Poisson brackets of two general functions  $A$  and  $B$  are defined as

$$\{A, B\}_D := \{A, B\} - \sum_{i,j=1}^2 \{A, G_i\} (M^{-1})_{ij} \{G_j, B\}. \quad (\text{A8})$$

The only nonvanishing Dirac brackets of position and momentum variables are

$$\{x, p_x\}_D = 1, \quad \{y, p_x\}_D = \frac{1}{1 + \beta \cos(y)}. \quad (\text{A9})$$

Having introduced the Dirac brackets, the weak equality signs in Eqs. (A2) and (A5) can be replaced by strong equality signs, keeping in mind that one must not work with the usual Poisson brackets but Dirac's version. As a consequence,  $x$  and  $p_y$  can be eliminated in the primary Hamiltonian in Eq. (A3), thus resulting in the final Hamiltonian

$$H = \frac{p_x^2}{2m} + \frac{\beta^2 \sin^2(y)}{2} - \beta \cos(y), \quad (\text{A10})$$

which is not branched but a function of nonsymplectic coordinates.

The classical Hamiltonian equations of motion for  $y$  and  $p_x$  are two coupled differential equations of first order and evaluate to

$$\dot{y} = \{y, H\}_D = \frac{p_x}{m[1 + \beta \cos(y)]}, \quad (\text{A11a})$$

$$\dot{p}_x = \{p_x, H\}_D = -\beta \sin(y). \quad (\text{A11b})$$

As a consistency check, they can be combined to obtain the second-order differential equation

$$m\ddot{y} = \frac{\beta \sin(y)}{1 + \beta \cos(y)} (m\dot{y}^2 - 1), \quad (\text{A12})$$

which coincides with the Euler-Lagrange equation of motion derived from the Lagrangian in Eq. (A1) after eliminating the  $x$  degree of freedom.

At this point, for  $\beta \geq 1$ , we note that the matrix  $M$  in Eq. (A6) is not invertible if

$$1 + \beta \cos(y) = 0, \quad (\text{A13})$$

which results in a singularity of the Dirac brackets in Eq. (A9). However, the values of  $y$  that satisfy the condition in Eq. (A13) correspond to critical values of the final Hamiltonian in Eq. (A10) [107] where the symplectic structure of phase space vanishes [108]. In fact, as the agreement of the classical Hamiltonian and Lagrangian equations of motion shows, such a singularity does not affect the validity of the Dirac-Bergmann algorithm.

Finally, we remark that one can also construct a single-valued Hamiltonian with a set of symplectic coordinates by introducing the new momentum

$$p = p_x[1 + \beta \cos(y)] \quad (\text{A14})$$

such that  $\{y, p\}_D = 1$ . Given these variables, however, the system is described by the Hamiltonian

$$H' = \frac{p^2}{2m(y)} + \frac{\beta^2 \sin^2(y)}{2} - \beta \cos(y), \quad (\text{A15})$$

which involves the position-dependent mass

$$m(y) = m[1 + \beta \cos(y)]^2 \quad (\text{A16})$$

that vanishes at  $1 + \beta \cos(y) = 0$ .

Similar to our approach in the main text in Sec. II B, here we do not attempt to provide a quantized theory for the system that is described by the Lagrangian in Eq. (A1). Despite the aforementioned singularities for  $\beta \geq 1$ , it turns out that the quantization of  $H$  in Eq. (A10) would require a systematic noncanonical quantization process, while  $H'$  in Eq. (A15) would need to be brought into a Hermitian form prior quantization. As we show in the main text, for the description of electrical networks, both of these procedures can be circumvented by removing the singularity of the initial Lagrangian.

## APPENDIX B: PROOFS OF THE THEOREMS

In this appendix, we collectively work out the proofs of the theorems that we present in Sec. III to demonstrate the failure of the Dirac-Bergmann algorithm. To this end, we provide two helpful lemmas.

**Lemma 1.** Suppose that a nonlinear inductor of type 1 is described by the potential  $U_{\text{NL}}(\phi_c)$ . Then, for some  $\gamma \in (0, 2)$  and all  $\phi_c$ ,

$$\forall \beta > 0 \exists M > 0: |U_{\text{NL}}(\phi_c)| \leq \beta |\phi_c|^\gamma + M.$$

*Proof.*—Fix  $\beta > 0$  for the remainder of the proof. From the definition of a nonlinear inductor of type 1, it follows that there exist some  $\gamma \in (0, 2)$  such that  $\lim_{|\phi_c| \rightarrow \infty} |U_{\text{NL}}(\phi_c)| / \beta |\phi_c|^\gamma = 0$ . Thus, there exists  $\tilde{\phi}_c \in \mathbb{R}^+$  such that  $|U_{\text{NL}}(\phi_c)| \leq \beta |\phi_c|^\gamma$  for all  $|\phi_c| \geq \tilde{\phi}_c$ . With  $M = \max_{\phi_c \in [-\tilde{\phi}_c, \tilde{\phi}_c]} |U_{\text{NL}}(\phi_c)|$ , the inequality  $|U_{\text{NL}}(\phi_c)| \leq \beta |\phi_c|^\gamma + M$  holds for all  $\phi_c \in \mathbb{R}$ . ■

In the next lemma, we introduce a new dynamical variable  $y$ , in anticipation of the rescaling that is done in the proof of the upcoming theorem:

**Lemma 2.** Suppose that two Hamiltonians  $H_1$  and  $H_2$  satisfy  $H_2 = H_1 + \delta V(y)$  with  $\delta V(y) \geq 0$  for all  $y$ . Then, the ground-state energies of  $H_1$  and  $H_2$  satisfy  $E_0(H_2) \geq E_0(H_1)$ .

*Proof.*—Let  $|\psi\rangle$  be the normalized ground state of  $H_2$ . Then, with the variational method applied to  $H_1$ , one obtains for the ground-state energy of  $H_2$ :

$$\begin{aligned} E_0(H_2) &= \langle \psi | H_2 | \psi \rangle \\ &= \langle \psi | H_1 | \psi \rangle + \langle \psi | \delta V(y) | \psi \rangle \geq E_0(H_1). \end{aligned} \quad (\text{B1})$$

Thus, the ground-state energy of  $H_2$  is lower bounded by the ground-state energy of  $H_1$ . ■

It follows that the ground-state energy of a particle in a potential  $V_2(y)$ , with  $y$  being the position variable, is always larger than or equal to the ground-state energy of the same particle in a potential  $V_1(y)$  if  $V_2(y) \geq V_1(y)$  for all values of  $y$ . Furthermore, suppose that a third Hamiltonian  $H_3$  satisfies  $H_3 = H_2 + \Delta V(y)$  with  $\Delta V(y) \geq 0$ . Then, using same reasoning, we obtain the useful ‘‘sandwich’’  $E_0(H_3) \geq E_0(H_2) \geq E_0(H_1)$ .

### 1. Proof of Theorem 1

We start with the proof of Theorem 1 in Sec. III B 1, which states that for a nonlinear inductor of type 1(a), the Born-Oppenheimer potential vanishes as  $C'/C \rightarrow 0$ .

*Proof.*—We introduce the  $LC'$ -resonator frequency and the flux zero-point fluctuation defined as

$$\omega'_r = \frac{1}{\sqrt{LC'}}, \quad \Phi_{\text{ZPF}} = \sqrt{\hbar} \sqrt[4]{\frac{L}{C'}}, \quad (\text{B2})$$

respectively, and we express  $H_{\text{fast}}$  as

$$H_{\text{fast}} = \hbar \omega'_r \left[ \frac{p_y^2 + (y - \phi/\Phi_{\text{ZPF}})^2}{2} + \frac{U_{\text{NL}}(y\Phi_{\text{ZPF}})}{\hbar \omega'_r} \right]. \quad (\text{B3})$$

The dimensionless conjugate variables  $y$  and  $p_y$  are defined as  $y = \phi_c/\Phi_{\text{ZPF}}$  and  $p_y = Q_c \Phi_{\text{ZPF}}/\hbar$ , and they satisfy the canonical commutation relation  $[y, p_y] = i$ .

We define the parameter  $\epsilon = 1/\sqrt{\hbar \omega'_r} = \sqrt{L}/\Phi_{\text{ZPF}}$ , and we divide out the prefactor in Eq. (B3), obtaining

$$\epsilon^2 H_{\text{fast}} = H_0 + \frac{\epsilon^2 \phi^2}{2L} - \frac{\epsilon \phi y}{\sqrt{L}} + \epsilon^2 U_{\text{NL}}(\sqrt{L}y/\epsilon), \quad (\text{B4})$$

with the dimensionless harmonic-oscillator Hamiltonian  $H_0 = (p_y^2 + y^2)/2$ . By definition of a type-1 inductor, there exists a parameter  $\gamma \in (0, 2)$  such that

$$\lim_{\epsilon \rightarrow 0} \epsilon^\gamma U_{\text{NL}}(\sqrt{L}y/\epsilon) = 0 \quad (\text{B5})$$

for all values of  $y$ . With this property of  $U_{\text{NL}}(\phi_c)$  in mind, we introduce the auxiliary Hamiltonian

$$\epsilon^2 H_{\text{aux}} = H_0 + \frac{\epsilon^2 \phi^2}{2L} - \frac{\epsilon \phi y}{\sqrt{L}} + \epsilon^{2-\gamma} \alpha^\gamma U_{\text{NL}}(\sqrt{L}y/\alpha), \quad (\text{B6})$$

which generalizes  $H_{\text{fast}}$  as it involves a new independent parameter  $\alpha$ . The fast Hamiltonian is recovered from the auxiliary one by setting  $\alpha = \epsilon$  as  $H_{\text{aux}} = H_{\text{fast}}$  in that case.

Without loss of generality, we choose  $\gamma \in \mathbb{Q}$ , and therefore, we set  $\gamma = p/q$  with  $p, q \in \mathbb{N}$  satisfying  $2q - p \in \mathbb{N}$ . We substitute  $\epsilon = \lambda^q$  in the auxiliary Hamiltonian to obtain

$$\lambda^{2q} H_{\text{aux}} = H_0 + \frac{\lambda^{2q} \phi^2}{2L} - \frac{\lambda^q \phi y}{\sqrt{L}} + \lambda^{2q-p} \alpha^\gamma U_{\text{NL}}(\sqrt{L}y/\alpha). \quad (\text{B7})$$

The operator domain  $D$  of  $\lambda^{2q} H_{\text{aux}}$  is independent of  $\lambda$ , and for each  $|\psi\rangle \in D$ ,  $\lambda^{2q} H_{\text{aux}} |\psi\rangle$  is a vector-valued analytic function of  $\lambda$ . Thus,  $\lambda^{2q} H_{\text{aux}}$  is an analytic family in the sense of Kato [in particular, an analytic family of type (A); see p. 16 in Ref. [48]] and the Kato-Rellich theorem applies; see p. 15, Theorem XII.8 in Ref. [48]. It follows that for any value of  $\phi$  and  $\alpha > 0$ , the  $n$ th eigenenergy  $\lambda^{2q} E_{\phi,n}(\lambda, \alpha)$  of  $\lambda^{2q} H_{\text{aux}}$  is an analytic function in  $\lambda$  with a nonvanishing radius of convergence  $\lambda_n(\phi, \alpha)$ ; i.e., for all  $\lambda < \lambda_n(\phi, \alpha)$  we can write the eigenenergy as Rayleigh-Schrödinger series (p. 1 in Ref. [48]):

$$\lambda^{2q} E_{\phi,n}(\lambda, \alpha) = \sum_{k=0}^{\infty} E_{\phi,n}^{(k)}(\alpha) \lambda^k. \quad (\text{B8})$$

By construction, and since the auxiliary Hamiltonian in Eq. (B7) is a polynomial in  $\phi$ , the Rayleigh-Schrödinger coefficients  $E_{\phi,n}^{(k)}(\alpha)$  are polynomials in  $\phi$  of the order  $j \leq k/q$ .

We have not yet established that the Rayleigh-Schrödinger coefficients are well behaved as  $\alpha \rightarrow 0$ . We now show this for the ground state: Consider the pair of new auxiliary Hamiltonians

$$\lambda^{2q} H^\pm = H_0 + \frac{\lambda^{2q} \phi^2}{2L} - \frac{\lambda^q \phi y}{\sqrt{L}} \pm \lambda^{2q-p} [\beta |\sqrt{L}y|^\gamma + \alpha^\gamma M], \quad (\text{B9})$$

with  $\beta, M > 0$ . Since  $\alpha^\gamma$  enters Eq. (B9) as the prefactor of the identity operator on the right-hand side, the eigenenergies  $\lambda^{2q} E_{\phi,n}^\pm(\lambda, \alpha)$  of  $\lambda^{2q} H^\pm$  depend linearly on  $\alpha^\gamma$ . According to Lemma 1, the parameters  $\beta$  and  $M$  can be chosen such that  $|U_{\text{NL}}(\phi_c)| \leq \beta |\phi_c|^\gamma + M$ , and therefore,  $\lambda^{2q}(H^+ - H_{\text{aux}}) \geq 0$ ,  $\lambda^{2q}(H_{\text{aux}} - H^-) \geq 0$ . Applying Lemma 2 twice gives

$$\lambda^{2q} E_{\phi,0}^-(\lambda, \alpha) \leq \lambda^{2q} E_{\phi,0}(\lambda, \alpha) \leq \lambda^{2q} E_{\phi,0}^+(\lambda, \alpha). \quad (\text{B10})$$

Furthermore, it follows from Sturm-Liouville theory and its extensions (p. 719ff in Ref. [109]) that  $|\lambda^{2q} E_{\phi,0}^\pm(\lambda, \alpha)| < \infty$ . Thus, the ground-state energy  $\lambda^{2q} E_{\phi,0}(\lambda, \alpha)$  remains finite for any  $\alpha < \infty$ , and, within the radius of convergence, the Rayleigh-Schrödinger coefficients satisfy  $\lim_{\alpha \rightarrow 0} |E_{\phi,0}^{(k)}(\alpha)| < \infty$ ; thus, these

coefficients are guaranteed to be “well behaved,” including when  $\alpha \rightarrow 0$ .

Since  $\lambda^{2q}H_{\text{aux}}$  is an analytic family of type (A), the radius of convergence of Eq. (B8)  $\lambda_n(\phi, \alpha)$  can be lower bounded (see p. 379, Remark 2.9 in Ref. [47]) by a function  $r_n(\phi, \alpha) > 0$  that remains finite as  $\alpha \rightarrow 0$  (in fact, it increases monotonically as  $\alpha$  decreases; see below). Thus, there exists  $\tilde{\alpha}_0(\phi) > 0$  such that

$$r_0(\phi, \tilde{\alpha}_0(\phi)) = \tilde{\alpha}_0(\phi)^{1/q} \equiv \tilde{\lambda}_0(\phi). \quad (\text{B11})$$

It follows that the Rayleigh-Schrödinger series in Eq. (B8) converges at least if  $\lambda < \tilde{\lambda}_0(\phi)$  and  $\alpha < \tilde{\alpha}_0(\phi)$ . Thus, for  $\lambda < \tilde{\lambda}_0(\phi)$ , the ground-state energy of  $\epsilon^2 H_{\text{fast}}$  is given by Eq. (B8) with the substitution  $\alpha = \lambda^q$ .

Because of the symmetry of  $U_{\text{NL}}(\phi_c)$  for nonlinear inductors of type 1(a), the eigenenergies  $\lambda^{2q}E_{\phi,n}(\lambda, \alpha)$  are symmetric in  $\phi$ , i.e.,

$$E_{\phi,n}(\lambda, \alpha) = E_{-\phi,n}(\lambda, \alpha) \quad (\text{B12})$$

for any value of  $\lambda$  and  $\alpha > 0$ . Thus, the Rayleigh-Schrödinger coefficients  $E_{\phi,n}^{(k)}(\alpha)$  must contain only even powers of  $\phi$ . It follows that  $E_{\phi,n}^{(k)}(\alpha) - E_{0,n}^{(k)}(\alpha) = 0$  for  $k < 2q$ . Thus, the Born-Oppenheimer potential as defined in Eq. (19) can be expressed as

$$\begin{aligned} U_{\text{BO}}(\phi) &= E_{\phi,0}(\lambda, \alpha) - E_{0,0}(\lambda, \alpha)|_{\alpha=\lambda^q} \\ &= \sum_{k=0}^{\infty} [E_{\phi,0}^{(2q+k)}(\lambda^q) - E_{0,0}^{(2q+k)}(\lambda^q)] \lambda^k. \end{aligned} \quad (\text{B13})$$

The limit of vanishingly small intrinsic capacitance  $C'$  corresponds to the limit  $\lambda \rightarrow 0$ . To analyze  $U_{\text{BO}}(\phi)$  in this limit, the addition and multiplication rules for limits as well as a straightforward evaluation of  $E_{\phi,0}^{(2q)}(\lambda^q)$  yield

$$\lim_{\lambda \rightarrow 0} U_{\text{BO}}(\phi) = \lim_{\lambda \rightarrow 0} [E_{\phi,0}^{(2q)}(\lambda^q) - E_{0,0}^{(2q)}(\lambda^q)] = 0. \quad (\text{B14})$$

Thus, for any value of  $\phi$ , the Born-Oppenheimer potential vanishes in the limit  $C' \rightarrow 0$ . ■

More information on analytic perturbation theory can be found in Refs. [106,110], supplementing the results we use directly in our proofs [47,48].

### a. Evaluation of the radius of convergence

The proof of Theorem 1 requires the Rayleigh-Schrödinger series in Eq. (B8) to converge. Here, we derive a lower bound of its radius of convergence  $\lambda_n(\phi, \alpha)$ . In the following, we consider all parameters and variables to be dimensionless, and we assume  $\phi \geq 0$ .

By definition, any analytic family of type (A) in the sense of Kato can be written as [47]

$$T(\lambda) = T + \lambda T^{(1)} + \lambda^2 T^{(2)} + \dots \quad (\text{B15})$$

with  $T$  being a closable operator with domain  $D$ , and  $T^{(k)}$  being operators with domains containing  $D$ . Furthermore, for any analytic family of type (A), there exist constants  $a, b, c > 0$  such that (see p. 378, Remark 2.8 in Ref. [47])

$$\|T^{(k)}u\| \leq c^{k-1}(a\|u\| + b\|Tu\|), \quad u \in D, \quad k \in \mathbb{N}. \quad (\text{B16})$$

A comparison of  $\lambda^{2q}H_{\text{aux}}$  in Eq. (B7) with Eq. (B15) identifies  $T = H_0$ ,  $T^{(k)} = 0$  for  $k \notin \{q, 2q, 2q-p\}$ , and

$$T^{(q)} = -\frac{y\phi}{\sqrt{L}}, \quad T^{(2q)} = \frac{\phi^2}{2L}, \quad T^{(2q-p)} = \alpha^\gamma U_{\text{NL}}\left(\frac{\sqrt{L}y}{\alpha}\right). \quad (\text{B17})$$

In the following, we show that each operator in Eq. (B17) is  $T$  bounded. As  $T^{(2q)} \propto 1$ , it follows trivially that

$$\|T^{(2q)}u\| \leq \frac{\phi^2}{2L}\|u\|. \quad (\text{B18})$$

For constants  $A, B > 0$  satisfying  $4AB \geq 1$ , the inequality  $|y| \leq A + By^2$  holds, and therefore (cf. Secs. II.1. and II.9. in Ref. [106]),

$$\|T^{(q)}u\| \leq \frac{\phi(A+2B)}{\sqrt{L}}\|u\| + \frac{2\phi B}{\sqrt{L}}\|Tu\|. \quad (\text{B19})$$

Recall that  $U_{\text{NL}}(\phi_c)$  describes a nonlinear inductor of type 1. Lemma 1 guarantees the existence of constants  $\beta, M > 0$  such that  $|U_{\text{NL}}(\phi_c)| \leq \beta|\phi_c|^\gamma + M$ . Furthermore, for  $\gamma \in (0, 2)$ , there exist constants  $A', B' > 0$  such that  $|y|^\gamma \leq B'y^2 + A'$ . It follows that

$$\begin{aligned} \|T^{(2q-p)}u\| &\leq [\alpha^\gamma M + L^{\gamma/2}\beta(A' + 2B')]\|u\| \\ &\quad + 2L^{\gamma/2}\beta B'\|Tu\|. \end{aligned} \quad (\text{B20})$$

Thus, the inequality in Eq. (B16) is satisfied with the choice

$$a = \max \left\{ \frac{\phi^2}{2L}, \frac{\phi(A+2B)}{\sqrt{L}}, \alpha^\gamma M + L^{\gamma/2}\beta(A' + 2B') \right\}, \quad (\text{B21})$$

$$b = \max \left\{ \frac{2\phi B}{\sqrt{L}}, 2L^{\gamma/2}\beta B' \right\}, \quad (\text{B22})$$

$$c = 1. \quad (\text{B23})$$

In the following, we set  $A = \phi/2\sqrt{L}$  and  $B = \sqrt{L}/2\phi$ . Furthermore, for any value of  $\phi$ , we can choose  $\beta$  such that  $a = \alpha^\gamma M + L^{\gamma/2}\beta(A' + 2B')$  and  $b = 2L^{\gamma/2}\beta B'$ . Note that  $a \equiv a(\alpha)$  increases monotonically as  $\alpha$  increases.

Following p. 379, Remark 2.9 in Ref. [47], the Rayleigh-Schrödinger series Eq. (B8) is convergent at least for

$$\lambda < \min_{\zeta \in \Gamma_n} [a \|R(\zeta)\| + b \|TR(\zeta)\| + c]^{-1}, \quad (\text{B24})$$

where  $\Gamma_n$  is a closed curve in the complex plane separating the  $n$ th eigenenergy of  $T$  from the rest of its spectrum and  $R(\zeta) = (T - \zeta)^{-1}$  is the resolvent of  $T$ .

Recall that  $T = H_0$  is the unperturbed harmonic-oscillator Hamiltonian with the spectrum  $n + 1/2$ ,  $n \in \mathbb{N}_0$ . We choose  $\Gamma_n$  to be a circle with radius  $1/2$  centered at  $n + 1/2$  such that  $\|R(\zeta)\| = 2$  for  $\zeta \in \Gamma_n$ . Moreover, for  $\zeta \in \Gamma_0$ , we find the inequality  $\|TR(\zeta)\| \leq 3$ . Thus, for the ground-state energy, the radius of convergence of the Rayleigh-Schrödinger series is lower bounded by

$$r_0(\phi, \alpha) = \frac{1}{2a(\alpha) + 3b + 1}, \quad (\text{B25})$$

which is always positive and increases as  $\alpha$  decreases.

## 2. Proof of Theorem 2

Next, we present the brief proof of Theorem 2 in Sec. III B 1, which complements Theorem 1 by considering nonlinear inductors of type 1(b).

*Proof.*—For nonlinear inductors of type 1(b), all arguments in the proof of Theorem 1 remain applicable until Eq. (B12), but the further argument cannot rely on the even parity of the eigenvalues with respect to  $\phi$ . For  $\gamma \in (0, 1)$ , an explicit and straightforward evaluation of the Rayleigh-Schrödinger coefficients shows that  $E_{\phi,n}^{(k)}(\alpha) - E_{0,n}^{(k)}(\alpha) = 0$  for  $k \leq 2q$  [111]. Thus, the Born-Oppenheimer potential can be expressed as in Eq. (B13), and Eq. (B14) remains valid. ■

## 3. Proof of Theorem 3

Here, we prove Theorem 3 in Sec. III B 2, which states that the Born-Oppenheimer potential approaches  $\phi^2/2L$  as  $C'/C \rightarrow 0$  if the nonlinear inductor is of type 2 with  $U_{\text{NL}}(\phi_c)$  as defined in Eq. (20).

*Proof.*—We introduce the pair of rescaled conjugate variables  $y = C'^{\frac{1}{\gamma+2}} \phi_c$  and  $p_y = Q_c / C'^{\frac{1}{\gamma+2}}$  satisfying the canonical commutation relation  $[y, p_y] = i\hbar$ . The Hamiltonian  $H_{\text{fast}}$  expressed in these variables reads

$$H_{\text{fast}} = C'^{-\frac{\gamma}{\gamma+2}} \left( \frac{p_y^2}{2} + \beta |y|^\gamma \right) + \frac{y^2}{2LC'^{\frac{2}{\gamma+2}}} - \frac{\phi y}{LC'^{\frac{1}{\gamma+2}}} + \frac{\phi^2}{2L}. \quad (\text{B26})$$

We define the Hamiltonian  $H_0 = p_y^2/2 + \beta |y|^\gamma$  and the parameter  $\epsilon = C'^{\frac{1}{\gamma+2}}$ . Multiplying Eq. (B26) with  $\epsilon^\gamma$  results in

$$\epsilon^\gamma H_{\text{fast}} = H_0 + \epsilon^{\gamma-2} \frac{y^2}{2L} - \epsilon^{\gamma-1} \frac{\phi y}{L} + \epsilon^\gamma \frac{\phi^2}{2L}. \quad (\text{B27})$$

Since  $\gamma \in \mathbb{Q}^{>2}$ , we set  $\gamma = p/q$  with  $p, q \in \mathbb{N}$  satisfying  $p - 2q \in \mathbb{N}$ . We substitute  $\epsilon = \lambda^q$  in the fast Hamiltonian and obtain

$$\lambda^p H_{\text{fast}} = H_0 + \lambda^{p-2q} \frac{y^2}{2L} - \lambda^{p-q} \frac{\phi y}{L} + \lambda^p \frac{\phi^2}{2L}, \quad (\text{B28})$$

which is an analytic family of type (A) in the sense of Kato. Since the spectrum of  $H_0$  is nondegenerate (p. 719ff in Ref. [109]), the Kato-Rellich theorem applies, and the  $n$ th eigenenergy of  $\lambda^p H_{\text{fast}}$  is an analytic function in  $\lambda$  with a nonvanishing radius of convergence  $\lambda_n(\phi) > 0$ ; i.e., for all  $\lambda < \lambda_n(\phi)$  we can write the eigenenergy as the Rayleigh-Schrödinger series

$$\lambda^p E_{\phi,n}(\lambda) = \sum_{k=0}^{\infty} E_{\phi,n}^{(k)} \lambda^k. \quad (\text{B29})$$

For  $k < p$ , the Rayleigh-Schrödinger coefficients  $E_{\phi,n}^{(k)}$  do not depend on  $\phi$ , and it follows that  $E_{\phi,n}^{(k)} - E_{0,n}^{(k)} = 0$  for  $k < p$ .

Within the radius of convergence, i.e., for  $\lambda < \lambda_0(\phi)$ , the Born-Oppenheimer potential as defined in Eq. (19) can be expressed as

$$U_{\text{BO}}(\phi) = E_{\phi,0}(\lambda) - E_{0,0}(\lambda) = \sum_{k=0}^{\infty} [E_{\phi,0}^{(p+k)} - E_{0,0}^{(p+k)}] \lambda^k. \quad (\text{B30})$$

The limit of vanishingly small intrinsic capacitance  $C'$  corresponds to the limit  $\lambda \rightarrow 0$ . To analyze  $U_{\text{BO}}(\phi)$  in this limit, the addition and multiplication rules for limits as well as a straightforward evaluation of  $E_{\phi,0}^{(p)}$  yield

$$\lim_{\lambda \rightarrow 0} U_{\text{BO}}(\phi) = E_{\phi,0}^{(p)} - E_{0,0}^{(p)} = \frac{\phi^2}{2L}. \quad (\text{B31})$$

Thus, for any value of  $\phi$ , the Born-Oppenheimer potential approaches the potential of the linear inductance  $L$  in the limit  $C' \rightarrow 0$ . ■

## 4. Proof of Theorem 4

Finally, we provide a proof of Theorem 4 in Sec. III B 3, stating that a quasilinear inductor can be considered linear in the limit  $C' \rightarrow 0$ . To show this, we combine ideas of the proofs of Theorems 1 and 3. In particular, with regard to the fast Hamiltonian in Eq. (16), we split the potential of the type- $L$  inductor into two parts, with one part rescaling the underlying harmonic-oscillator Hamiltonian, while the

other part is identified as contribution to the perturbation of that system.

*Proof.*—It follows from the definition of a type- $L$  nonlinear inductor that there exists a constant  $\mathfrak{L} > 0$  such that its potential can be written as

$$U_{\text{NL}}(\phi_c) = \frac{\phi_c^2}{2\mathfrak{L}} + U_{\text{I1}}(\phi_c), \quad (\text{B32})$$

where  $U_{\text{I1}}(\phi_c)$  describes a nonlinear inductor of type 1. We define the effective parallel combination inductance  $l$  and the characteristic flux scale  $\Phi$  as

$$l = \frac{L\mathfrak{L}}{L + \mathfrak{L}}, \quad \Phi = \sqrt{\hbar} \sqrt[4]{\frac{l}{C}}, \quad (\text{B33})$$

respectively. We further introduce the dimensionless conjugate variables  $y = \phi_c/\Phi$  and  $p_y = Q_c\Phi/\hbar$  satisfying the canonical commutation relation  $[y, p_y] = i$ .

With  $\epsilon = \sqrt{l}/\Phi$  and  $H_0 = (p_y^2 + y^2)/2$ , the fast Hamiltonian in Eq. (16) can be expressed as [cf. Eq. (B4)]

$$\epsilon^2 H_{\text{fast}} = H_0 + \frac{\epsilon^2 \phi^2}{2L} - \frac{\epsilon \sqrt{l} \phi y}{L} + \epsilon^2 U_{\text{I1}}(\sqrt{l}y/\epsilon). \quad (\text{B34})$$

For the remainder of this proof, all arguments in the proofs of Theorem 1 for nonlinear inductors of type 1(a) and Theorem 2 for nonlinear inductors of type 1(b) remain applicable until Eq. (B14). In particular, the Born-Oppenheimer potential can be expressed as in Eq. (B13). However, as opposed to type-1 nonlinear inductors, here, a straightforward evaluation of  $E_{\phi,0}^{(2q)}(\lambda^q)$  yields

$$\lim_{\lambda \rightarrow 0} U_{\text{BO}}(\phi) = \lim_{\lambda \rightarrow 0} [E_{\phi,0}^{(2q)}(\lambda^q) - E_{0,0}^{(2q)}(\lambda^q)] = \frac{\phi^2}{2(L + \mathfrak{L})}. \quad (\text{B35})$$

Thus, for any value of  $\phi$ , the Born-Oppenheimer potential approaches the potential of a linear inductance  $L + \mathfrak{L}$  in the limit  $C' \rightarrow 0$ . ■

---

[1] R. P. Feynman, *Simulating Physics with Computers*, *Int. J. Theor. Phys.* **21**, 467 (1982).  
 [2] M. A. Nielsen and I. L. Chuang, *Quantum Computation and Quantum Information: 10th Anniversary Edition* (Cambridge University Press, Cambridge, England, 2010).  
 [3] F. Arute, K. Arya, R. Babbush *et al.*, *Quantum Supremacy Using a Programmable Superconducting Processor*, *Nature (London)* **574**, 505 (2019).  
 [4] Y. Wu, Wan-Su Bao, Sirui Cao *et al.*, *Strong Quantum Computational Advantage Using a Superconducting Quantum Processor*, *Phys. Rev. Lett.* **127**, 180501 (2021).

[5] Qingling Zhu, Sirui Cao, Fusheng Chen *et al.*, *Quantum Computational Advantage via 60-Qubit 24-Cycle Random Circuit Sampling*, *Sci. Bull.* **67**, 240 (2022).  
 [6] A. Shnirman, G. Schön, and Z. Hermon, *Quantum Manipulations of Small Josephson Junctions*, *Phys. Rev. Lett.* **79**, 2371 (1997).  
 [7] V. Bouchiat, D. Vion, P. Joyez, D. Esteve, and M. H. Devoret, *Quantum Coherence with a Single Cooper Pair*, *Phys. Scr. T* **76**, 165 (1998).  
 [8] Y. Nakamura, Y. A. Pashkin, and J. S. Tsai, *Coherent Control of Macroscopic Quantum States in a Single-Cooper-Pair Box*, *Nature (London)* **398**, 786 (1999).  
 [9] J. Preskill, *Quantum Computing in the NISQ Era and Beyond*, *Quantum* **2**, 79 (2018).  
 [10] A. Kitaev, *Protected Qubit Based on a Superconducting Current Mirror*, [arXiv:cond-mat/0609441v2](https://arxiv.org/abs/cond-mat/0609441v2).  
 [11] P. Brooks, A. Kitaev, and J. Preskill, *Protected Gates for Superconducting Qubits*, *Phys. Rev. A* **87**, 052306 (2013).  
 [12] J. M. Dempster, B. Fu, D. G. Ferguson, D. I. Schuster, and J. Koch, *Understanding Degenerate Ground States of a Protected Quantum Circuit in the Presence of Disorder*, *Phys. Rev. B* **90**, 094518 (2014).  
 [13] P. Groszkowski, A. D. Paolo, A. L. Grimsmo, A. Blais, D. I. Schuster, A. A. Houck, and J. Koch, *Coherence Properties of the 0- $\pi$  Qubit*, *New J. Phys.* **20**, 043053 (2018).  
 [14] A. Di Paolo, A. L. Grimsmo, P. Groszkowski, J. Koch, and A. Blais, *Control and Coherence Time Enhancement of the 0- $\pi$  Qubit*, *New J. Phys.* **21**, 043002 (2019).  
 [15] A. Gyenis, P. S. Mundada, A. Di Paolo, T. M. Hazard, X. You, D. I. Schuster, J. Koch, A. Blais, and A. A. Houck, *Experimental Realization of a Protected Superconducting Circuit Derived from the 0- $\pi$  Qubit*, *PRX Quantum* **2**, 010339 (2021).  
 [16] M. Devoret, *Quantum Fluctuations in Electrical Circuits*, in *Quantum Fluctuations*, edited by S. Reynaud, E. Giacobino, and J. Zinn-Justin (Elsevier, Amsterdam, 1997).  
 [17] U. Vool and M. Devoret, *Introduction to Quantum Electromagnetic Circuits*, *Int. J. Circuit Theory Appl.* **45**, 897 (2017).  
 [18] S. M. Girvin, *Circuit QED: Superconducting Qubits Coupled to Microwave Photons*, in *Quantum Machines: Measurement and Control of Engineered Quantum Systems*, edited by M. Devoret, B. Huard, R. Schoelkopf, and L. F. Cugliandolo (Oxford University Press, New York, 2014), pp. 113–256.  
 [19] A. Blais, A. L. Grimsmo, S. M. Girvin, and A. Wallraff, *Circuit Quantum Electrodynamics*, *Rev. Mod. Phys.* **93**, 025005 (2021).  
 [20] A. Gyenis, A. Di Paolo, J. Koch, A. Blais, A. A. Houck, and D. I. Schuster, *Moving beyond the Transmon: Noise-Protected Superconducting Quantum Circuits*, *PRX Quantum* **2**, 030101 (2021).  
 [21] T. E. Roth, R. Ma, and W. C. Chew, *An Introduction to the Transmon Qubit for Electromagnetic Engineers*, [arXiv:2106.11352](https://arxiv.org/abs/2106.11352).  
 [22] V. E. Manucharyan, J. Koch, L. I. Glazman, and M. H. Devoret, *Fluxonium: Single Cooper-Pair Circuit Free of Charge Offsets*, *Science* **326**, 113 (2009).  
 [23] G. Viola and G. Catelani, *Collective Modes in the Fluxonium Qubit*, *Phys. Rev. B* **92**, 224511 (2015).

- [24] N. A. Masluk, I. M. Pop, A. Kamal, Z. K. Mineev, and M. H. Devoret, *Microwave Characterization of Josephson Junction Arrays: Implementing a Low Loss Superinductance*, *Phys. Rev. Lett.* **109**, 137002 (2012).
- [25] L. Grünhaupt, M. Spiecker, D. Gusenkova, N. Maleeva, S. T. Skacel, I. Takmakov, F. Valenti, P. Winkel, H. Rotzinger, W. Wernsdorfer, A. V. Ustinov, and I. M. Pop, *Granular Aluminium as a Superconducting Material for High-Impedance Quantum Circuits*, *Nat. Mater.* **18**, 816 (2019).
- [26] M. Peruzzo, F. Hassani, G. Szep, A. Trioni, E. Redchenko, M. Žemlička, and J. M. Fink, *Geometric Superinductance Qubits: Controlling Phase Delocalization across a Single Josephson Junction*, *PRX Quantum* **2**, 040341 (2021).
- [27] N. E. Frattini, U. Vool, S. Shankar, A. Narla, K. M. Sliwa, and M. H. Devoret, *3-Wave Mixing Josephson Dipole Element*, *Appl. Phys. Lett.* **110**, 222603 (2017).
- [28] N. E. Frattini, V. V. Sivak, A. Lingenfelter, S. Shankar, and M. H. Devoret, *Optimizing the Nonlinearity and Dissipation of a SNAIL Parametric Amplifier for Dynamic Range*, *Phys. Rev. Appl.* **10**, 054020 (2018).
- [29] V. V. Sivak, N. E. Frattini, V. R. Joshi, A. Lingenfelter, S. Shankar, and M. H. Devoret, *Kerr-Free Three-Wave Mixing in Superconducting Quantum Circuits*, *Phys. Rev. Appl.* **11**, 054060 (2019).
- [30] S. P. Chitta, T. Zhao, Z. Huang, I. Mondragon-Shem, and J. Koch, *Computer-Aided Quantization and Numerical Analysis of Superconducting Circuits*, *New J. Phys.* **24**, 103020 (2022).
- [31] P. G. Bergmann, *Non-Linear Field Theories*, *Phys. Rev.* **75**, 680 (1949).
- [32] P. G. Bergmann and J. H. M. Brunings, *Non-Linear Field Theories II. Canonical Equations and Quantization*, *Rev. Mod. Phys.* **21**, 480 (1949).
- [33] P. A. M. Dirac, *Generalized Hamiltonian Dynamics*, *Can. J. Math.* **2**, 129 (1950).
- [34] J. L. Anderson and P. G. Bergmann, *Constraints in Covariant Field Theories*, *Phys. Rev.* **83**, 1018 (1951).
- [35] P. A. M. Dirac, *Generalized Hamiltonian Dynamics*, *Proc. R. Soc. A* **246**, 326 (1958).
- [36] P. A. M. Dirac, *Lectures on Quantum Mechanics* (Dover Publications, New York, 2001).
- [37] M. Henneaux and C. Teitelboim, *Quantization of Gauge Systems* (Princeton University Press, Princeton, NJ, 1992).
- [38] H. J. Rothe and K. D. Rothe, *Classical and Quantum Dynamics of Constrained Hamiltonian Systems* (World Scientific, Singapore, 2010).
- [39] J. D. Brown, *Singular Lagrangians, Constrained Hamiltonian Systems and Gauge Invariance: An Example of the Dirac-Bergmann Algorithm*, *Universe* **8**, 171 (2022).
- [40] M. Henneaux, C. Teitelboim, and J. Zanelli, *Quantum Mechanics for Multivalued Hamiltonians*, *Phys. Rev. A* **36**, 4417 (1987).
- [41] A. Shapere and F. Wilczek, *Branched Quantization*, *Phys. Rev. Lett.* **109**, 200402 (2012).
- [42] B. Peikari, *Fundamentals of Network Analysis and Synthesis* (Prentice-Hall, Englewood Cliffs, NJ, 1974).
- [43] L. O. Chua, C. A. Desoer, and E. S. Kuh, *Linear and Nonlinear Circuits* (McGraw-Hill College, New York, 1987).
- [44] C. A. Desoer and E. S. Kuh, *Basic Circuit Theory* (McGraw-Hill International Book Company, New York, 1969).
- [45] When a flux-controlled inductor has a characteristic  $f(\cdot)$  that is periodic in  $\phi$ , it may be appropriate (and important for quantization) to consider  $\phi$  to be a compact rather than extended variable [46]. This subtle issue does not affect any of the conclusions of this paper, and we do not consider the compactness question any further here.
- [46] J. Koch, V. Manucharyan, M. H. Devoret, and L. I. Glazman, *Charging Effects in the Inductively Shunted Josephson Junction*, *Phys. Rev. Lett.* **103**, 217004 (2009).
- [47] T. Kato, *Perturbation Theory for Linear Operators* (Springer, New York, 1995).
- [48] M. Reed and B. Simon, *Methods of Modern Mathematical Physics. IV Analysis of Operators* (Academic Press, New York, 1978).
- [49] There are exceptions to this rule. For example, ideal transformers do not enter the Lagrangian of a system as an additional term but enforce a constraint on the variables; see F. Solgun and D. P. DiVincenzo, *Multipoint Impedance Quantization*, *Ann. Phys. (Amsterdam)* **361**, 605 (2015).
- [50] Typically, the derivation of a Hamiltonian describing a superconducting circuit involves the inversion of a capacitance matrix, which conventional textbooks usually assume to be accomplishable.
- [51] We note that an alternatively proposed procedure—the Faddeev-Jackiw method [38,52], which is equivalent to the Dirac-Bergmann algorithm [53,54]—promises a simplified approach as no classification of constraints is required. In this paper, however, we work with the Dirac-Bergmann algorithm as its application turns out to be straightforward for our systems.
- [52] L. Faddeev and R. Jackiw, *Hamiltonian Reduction of Unconstrained and Constrained Systems*, *Phys. Rev. Lett.* **60**, 1692 (1988).
- [53] J. A. García and J. M. Pons, *Equivalence of Faddeev-Jackiw and Dirac Approaches for Gauge Theories*, *Int. J. Mod. Phys. A* **12**, 451 (1997).
- [54] L. Liao and Y. C. Huang, *Non-Equivalence of Faddeev-Jackiw Method and Dirac-Bergmann Algorithm and the Modification of Faddeev-Jackiw Method for Keeping the Equivalence*, *Ann. Phys. (Amsterdam)* **322**, 2469 (2007).
- [55] Note that different approaches of circuit quantization might also involve loop charges or mixtures of both sets of variables; see Ref. [56]. We note that the singularity of a system might depend on the chosen set of variables describing the system.
- [56] J. Ulrich and F. Hassler, *Dual Approach to Circuit Quantization Using Loop Charges*, *Phys. Rev. B* **94**, 094505 (2016).
- [57] M. Rymarz, *The Quantum Electrodynamics of Singular and Nonreciprocal Superconducting Circuits*, master's thesis, RWTH Aachen University, 2018.
- [58] M. Rymarz, *Nonreciprocal Circuit Quantization in the Singular Limit—Design of a Passively Protected Superconducting Qubit Encoding a Quantum Error-Correcting Code*, Ph.D. thesis, RWTH Aachen University (to be published).

- [59] J. Clarke and A. I. Braginski, *The SQUID Handbook: Applications of SQUIDs and SQUID Systems* (John Wiley & Sons, New York, 2006).
- [60] Z. K. Mineev, Z. Leghtas, S. O. Mundhada, L. Christakis, I. M. Pop, and M. H. Devoret, *Energy-Participation Quantization of Josephson Circuits*, arXiv:2010.00620v3.
- [61] S. Richer, N. Maleeva, S. T. Skacel, I. M. Pop, and D. DiVincenzo, *Inductively Shunted Transmon Qubit with Tunable Transverse and Longitudinal Coupling*, *Phys. Rev. B* **96**, 174520 (2017).
- [62] C. Teitelboim and J. Zanelli, *Dimensionally Continued Topological Gravitation Theory in Hamiltonian Form*, *Classical Quantum Gravity* **4**, L125 (1987).
- [63] A. Shapere and F. Wilczek, *Classical Time Crystals*, *Phys. Rev. Lett.* **109**, 160402 (2012).
- [64] Working with flux variables as generalized positions, the parasitic capacitance of an inductive element adds a term to the Lagrangian that is quadratic in the generalized velocity. This is basically equivalent to adding a mass to an otherwise massless particle, which, of course, is not a correct step in all physical theories.
- [65] G. Burkard, R. H. Koch, and D. P. DiVincenzo, *Multilevel Quantum Description of Decoherence in Superconducting Qubits*, *Phys. Rev. B* **69**, 064503 (2004).
- [66] M. Born and R. Oppenheimer, *Zur Quantentheorie der Molekeln*, *Ann. Phys. (Berlin)* **389**, 457 (1927).
- [67] D. P. DiVincenzo, F. Brito, and R. H. Koch, *Decoherence Rates in Complex Josephson Qubit Circuits*, *Phys. Rev. B* **74**, 014514 (2006).
- [68] In the molecular physics literature,  $H_{\text{fast}}$  is called the electronic Hamiltonian as it describes the motion of the fast (light) electrons for fixed positions of the slow (heavy) nuclei.
- [69] These definitions are structured to exclude from consideration potential functions that deviate very slowly from a linear inductance, e.g.,  $U_{\text{NL}}(\phi_c) \sim \phi_c^2 / \log(\phi_c^2 + 4)$ . We suspect that this potential behaves like a type-1 case, but the proofs of our theorems do not apply. Note that such functions are also excluded by the second part of the definition of type- $L$  inductors.
- [70] Sublinear and superlinear refer to the form of the classical two-terminal current-versus-flux characteristic. When this relation is linear, the coefficient of proportionality is an inverse inductance referred to as a reluctance in the electrical literature.
- [71] A. A. Golubov, M. Yu. Kupriyanov, and E. Il'ichev, *The Current-Phase Relation in Josephson Junctions*, *Rev. Mod. Phys.* **76**, 411 (2004).
- [72] Alexei Kitaev, *Protected Qubit Based on Superconducting Current Mirror*, U.S. Patent No. 7,858,966 (2010).
- [73] M. T. Bell, I. A. Sadovskyy, L. B. Ioffe, A. Yu. Kitaev, and M. E. Gershenson, *Quantum Superinductor with Tunable Nonlinearity*, *Phys. Rev. Lett.* **109**, 137003 (2012).
- [74] Carles Altimiras, Olivier Parlavecchio, Philippe Joyez, Denis Vion, Patrice Roche, Daniel Esteve, and Fabien Portier, *Tunable Microwave Impedance Matching to a High Impedance Source Using a Josephson Metamaterial*, *Appl. Phys. Lett.* **103**, 212601 (2013).
- [75] Xin Wang, Ya-Fen Lin, Jia-Qi Li, Wen-Xiao Liu, and Hong-Rong Li, *Chiral SQUID-Metamaterial Waveguide for Circuit-QED*, *New J. Phys.* **24**, 123010 (2022).
- [76] K. Kalashnikov, W. T. Hsieh, W. Zhang, W.-S. Lu, P. Kamenov, A. Di Paolo, A. Blais, M. E. Gershenson, and M. Bell, *Bifluxon: Fluxon-Parity-Protected Superconducting Qubit*, *PRX Quantum* **1**, 010307 (2020).
- [77] Long B. Nguyen, Gerwin Koolstra, Yosep Kim, Alexis Morvan, Trevor Chistolini, Shraddha Singh, Konstantin N. Nesterov, Christian Jünger, Larry Chen, Zahra Pedramrazi, Bradley K. Mitchell, John Mark Kreikebaum, Shruti Puri, David I. Santiago, and Irfan Siddiqi, *Blueprint for a High-Performance Fluxonium Quantum Processor*, *PRX Quantum* **3**, 037001 (2022).
- [78] Yinqi Chen, Konstantin N. Nesterov, Vladimir E. Manucharyan, and Maxim G. Vavilov, *Fast Flux Entangling Gate for Fluxonium Circuits*, *Phys. Rev. Appl.* **18**, 034027 (2022).
- [79] J. E. Mooij, T. P. Orlando, L. Levitov, Lin Tian, Caspar H. Van der Wal, and Seth Lloyd, *Josephson Persistent-Current qubit*, *Science* **285**, 1036 (1999).
- [80] T. P. Orlando, J. E. Mooij, Lin Tian, Caspar H. Van Der Wal, L. S. Levitov, Seth Lloyd, and J. J. Mazo, *Superconducting Persistent-Current Qubit*, *Phys. Rev. B* **60**, 15398 (1999).
- [81] Anthony J. Leggett, *Quantum Liquids: Bose Condensation and Cooper Pairing in Condensed-Matter Systems* (Oxford University Press, New York, 2006).
- [82] D. V. Averin and K. K. Likharev, *Coulomb Blockade of Single-Electron Tunneling, and Coherent Oscillations in Small Tunnel Junctions*, *J. Low Temp. Phys.* **62**, 345 (1986).
- [83] H. S. J. van der Zant, W. J. Elion, L. J. Geerligs, and J. E. Mooij, *Quantum Phase Transitions in Two Dimensions: Experiments in Josephson-Junction Arrays*, *Phys. Rev. B* **54**, 10081 (1996).
- [84] A. Noguchi, A. Osada, S. Masuda, S. Kono, K. Heya, S. P. Wolski, H. Takahashi, T. Sugiyama, D. Lachance-Quirion, and Y. Nakamura, *Fast Parametric Two-Qubit Gates with Suppressed Residual Interaction Using the Second-Order Nonlinearity of a Cubic Transmon*, *Phys. Rev. A* **102**, 062408 (2020).
- [85] Although SNAILS are mostly operated with  $N = 3$  large Josephson junctions, we focus on the case  $N = 2$  for the sake of simplicity.
- [86] J. Koch, T. M. Yu, J. Gambetta, A. A. Houck, D. I. Schuster, J. Majer, A. Blais, M. H. Devoret, S. M. Girvin, and R. J. Schoelkopf, *Charge-Insensitive Qubit Design Derived from the Cooper Pair Box*, *Phys. Rev. A* **76**, 042319 (2007).
- [87] A similar renormalization of the Josephson energy also occurs in the analysis of nonreciprocal circuits; see Ref. [88].
- [88] M. Rymarz, S. Bosco, A. Ciani, and D. P. DiVincenzo, *Hardware-Encoding Grid States in a Nonreciprocal Superconducting Circuit*, *Phys. Rev. X* **11**, 011032 (2021).
- [89] A. Di Paolo, T. E. Baker, A. Foley, D. Sénéchal, and A. Blais, *Efficient Modeling of Superconducting Quantum Circuits with Tensor Networks*, *npj Quantum Inf.* **7**, 11 (2021).
- [90] Note that the boundary conditions in Eq. (43) imply a preceding unitary gauge transformation of the initial wave function as the offset charges  $\nu_1, \nu_2$  do not enter the Hamiltonian in Eq. (31).

- [91] C. L. Kane and M. P. A. Fisher, *Transport in a One-Channel Luttinger Liquid*, *Phys. Rev. Lett.* **68**, 1220 (1992).
- [92] T. Fang, A. Konar, H. Xing, and D. Jena, *Carrier Statistics and Quantum Capacitance of Graphene Sheets and Ribbons*, *Appl. Phys. Lett.* **91**, 092109 (2007).
- [93] J. Xia, F. Chen, J. Li, and N. Tao, *Measurement of the Quantum Capacitance of Graphene*, *Nat. Nanotechnol.* **4**, 505 (2009).
- [94] S. Dröscher, P. Roulleau, F. Molitor, P. Studerus, C. Stampfer, K. Ensslin, and T. Ihn, *Quantum Capacitance and Density of States of Graphene*, *Appl. Phys. Lett.* **96**, 152104 (2010).
- [95] D. T. Le, A. Grimsmo, C. Müller, and T. M. Stace, *Doubly Nonlinear Superconducting Qubit*, *Phys. Rev. A* **100**, 062321 (2019).
- [96] B. Tellegen, *The Gyrator, a New Electric Network Element*, *Philips Res. Rep.* **3**, 81 (1948).
- [97] E. I. Rosenthal, B. J. Chapman, A. P. Higginbotham, J. Kerckhoff, and K. W. Lehnert, *Breaking Lorentz Reciprocity with Frequency Conversion and Delay*, *Phys. Rev. Lett.* **119**, 147703 (2017).
- [98] B. J. Chapman, E. I. Rosenthal, J. Kerckhoff, B. A. Moores, L. R. Vale, J. A. B. Mates, G. C. Hilton, K. Lalumière, A. Blais, and K. W. Lehnert, *Widely Tunable On-Chip Microwave Circulator for Superconducting Quantum Circuits*, *Phys. Rev. X* **7**, 041043 (2017).
- [99] F. Lecocq, L. Ranzani, G. A. Peterson, K. Cicak, R. W. Simmonds, J. D. Teufel, and J. Aumentado, *Nonreciprocal Josephson Amplifier*, *Phys. Rev. Appl.* **7**, 024028 (2017).
- [100] S. Barzanjeh, M. Wulf, M. Peruzzo, M. Kalaei, P. B. Dieterle, O. Painter, and J. M. Fink, *Mechanical On-Chip Microwave Circulator*, *Nat. Commun.* **8**, 953 (2017).
- [101] A. C. Mahoney, J. I. Colless, S. J. Pauka, J. M. Hornibrook, J. D. Watson, G. C. Gardner, M. J. Manfra, A. C. Doherty, and D. J. Reilly, *On-Chip Microwave Quantum Hall Circulator*, *Phys. Rev. X* **7**, 011007 (2017).
- [102] D. J. Parker, M. Savvitskyi, W. Vine, A. Laucht, T. Duty, A. Morello, A. L. Grimsmo, and J. J. Pla, *Degenerate Parametric Amplification via Three-Wave Mixing Using Kinetic Inductance*, *Phys. Rev. Appl.* **17**, 034064 (2022).
- [103] J. Ku, V. Manucharyan, and A. Bezryadin, *Superconducting Nanowires as Nonlinear Inductive Elements for Qubits*, *Phys. Rev. B* **82**, 134518 (2010).
- [104] S. Khorasani and A. Koottandavida, *Nonlinear Graphene Quantum Capacitors for Electro-Optics*, *npj 2D Mater. Appl.* **1**, 7 (2017).
- [105] S. Khorasani, *CUBIT: Capacitive qQuantum BIT*, *J. Carbon Res.* **4**, 39 (2018).
- [106] B. Simon and A. Dicke, *Coupling Constant Analyticity for the Anharmonic Oscillator*, *Ann. Phys. (N.Y.)* **58**, 76 (1970).
- [107] The critical values of the final Hamiltonian in Eq. (A10) coincide with those of the secondary constraint  $x(y) = y + \beta \sin(y)$  [cf. Eq. (A5)]. Therefore, these values correspond to the branching points of the multivalued potential.
- [108] L. Zhao, P. Yu, and W. Xu, *Hamiltonian Description of Singular Lagrangian Systems with Spontaneously Broken Time Translation Symmetry*, *Mod. Phys. Lett. A* **28**, 1350002 (2013).
- [109] P. M. Morse and H. Feshbach, *Methods of Theoretical Physics*, International Series in Pure and Applied Physics (McGraw-Hill, New York, 1953).
- [110] B. Simon, *Large Orders and Summability of Eigenvalue Perturbation Theory: A Mathematical Overview*, *Int. J. Quantum Chem.* **21**, 3 (1982).
- [111] Assume  $H = H_0 + \lambda^{2q}A + \lambda^q B + \lambda^{2q-p}C$  to be an analytic family in the sense of Kato, where the operators  $H_0, A, B, C$  do not depend on  $\lambda$ . Then, within some finite radius of convergence, the Rayleigh-Schrödinger series is analytic in  $\lambda$ , and the only powers of  $\lambda$  are given by  $k = i(2q) + j(q) + l(2q - p)$  with  $i, j, l \in \mathbb{N}_0$ . Thus, with  $q < 2q - p < 2q$ , there are only four possible values of  $k$  such that  $k \leq 2q$ .